3 Phase II: Production rate in the packed bed of the Ifcon process

3.1 Background

3.1.1 Objective

The origin of the Ifcon process was based on results from an experiment[18] that showed that 80% reduction could be achieved in a solids bed, at a material mixture feed rate of 135 kg/m^2/h. This correlated with an iron feed rate of about 60 kg Fe/m^2/h (and a production rate of 56 kg Fe/m^2/h [17]). Based on the result of 80% reduction achieved in the solids bed, it was assumed that the reduced bed is melted from below to produce metal and slag. In practice however, reduction can occur as a combination of solid-state reduction in the solids bed and solid-liquid-state reduction in the slag [1,17]:

The objective of this part of the study was to determine the extent of reduction achieved as solid-state reduction. For this, the following was done:

- Information from related studies was investigated.
- A kinetic model was used to predict the temperature profile and reduction profile through the solids bed.
- Experimental data was used to determine the applicable rate constants to be used in the model.
- The temperature profile through a solids bed was measured and compared to model predictions.
- Finally, the model was used to calculate the extent of reduction achieved, as solid-state reduction, in the solids bed.

3.1.2 Related studies and test approach

This investigation was done in conjunction with another study[19]. Both studies aimed at gaining information that complimented each other.

In the other study[19], the degree of reduction achieved (in the upper part of the solids bed) was estimated as a function of exposure time. For this, typical Ifcon-material-mixtures were exposed to elevated temperatures in a muffle furnace. Conditions in this muffle furnace simulated conditions in the freeboard of the Ifcon

process. The material mixtures were contained in identical alumina fibre crucibles that insulated the samples from all sides but one. The open end of each crucible was exposed to the muffle furnace (at an elevated temperature), for a specific time. After exposure, the degree of reduction achieved was determined for each sample. Results for 40 mm thick samples exposed to 1500°C are shown in ***Figure 29.*** The size of each sample was known and so was the time for which the sample was exposed. The cross-sectional area of each sample was also known. When the mass of the sample is divided by the time of exposure and the cross-sectional area, a specific feed rate (with units: $kg/m^2/h$) is obtained. Once the Fe content of the material mixture is known and a Fe yield is estimated, the feed rate can be expressed as a production rate. The results of the abovementioned investigation[19] were expressed in terms of production rate, rather than exposure time.

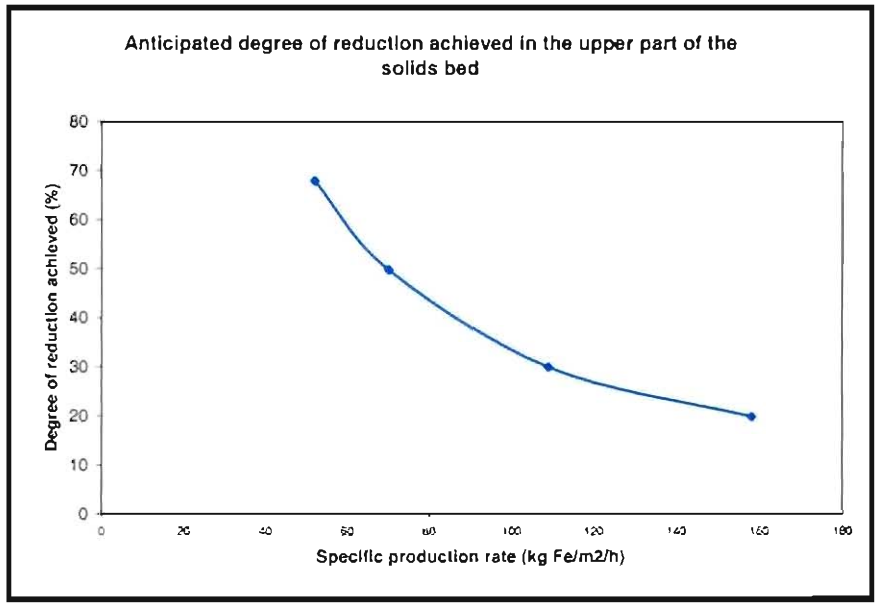

Figure 29 : *Results from muffle furnace experiments showing the anticipated degree of reduction achieved in the top 40 mm of the solids bed, as a function of production rate, for a freeboard temperature of 1500°C*[19].

As discussed in ***paragraph 1.4.2***, the solids bed can conceptually be divided into a top and bottom part, so that the top part only receives energy from above the solids bed, while the bottom part only receives energy from below the solids bed. ***Figure 29*** shows the anticipated degree of reduction in the top part of the solids bed, which was driven by energy from above the solids bed. Since the material that is partially reduced in the upper part of the solids bed, descends to the bottom part of the bed,

Figure 29 also shows the anticipated degree of reduction of material that enters the bottom part of the solids bed, as a function of production rate. This study investigated the rate at which partially reduced material, which entered the bottom part of the solids bed, was reduced by solid-state reduction.

The achievable production rate was calculated using a kinetic model (discussed in the next paragraph). To confirm model predictions, the results were tested experimentally.

Figure 29 shows that between 20% and 68% reduction can be achieved in the upper part of the solids bed. Data obtained from pilot plant campaigns[12] showed that the degree of reduction achieved on the outer surface of the solids bed was about 30%[12]. Accordingly, a material mixture containing 30 % pre-reduced iron ore was used as input material during the experimental investigation. Material mixtures containing 0% and 50% pre-reduced iron ore was also used as input material to test the sensitivity of the results. The experimental investigation is discussed in detail in ***paragraph 4.4***.

The production rate was also varied during the experimental investigation. Production rates of 30, 80 and 120 kg Fe/m^2/h were aimed for. This was done by varying the electrical energy input to the experimental set-up. The experimental procedure is described in detail in ***paragraph 3.4***. ***Table 4*** summarizes the experiments that were planned for this investigation.

Table 4: *Experimental program of phase II of the investigation*

Specific Production rate (kg Fe/m^2/h)	% Pre-reduction		
	0 %	30 %	50 %
30	X	X	X
80		X	
120		X	

The temperature profile that was predicted by the model was compared to experimentally measured temperature profiles. Point-counts were also done on

selected samples to identify the amounts of phases present at specific positions in the solids bed. This was done as reference to model predictions.

3.1.3 Other relevant studies

Huang and Lu[23] exposed ore–coal mixtures to 1200°C while measuring the temperature profile through the mixed burden. Their results indicated temperature gradients of between 10 and 40°C/mm.

Sun and Lu[39] also measured the temperature profiles through composite ore-coal mixtures. They found that the temperature gradients are steeper near the hot surface and for shorter reaction times (lower degrees of metallization). They also suggested that the low effective thermal conductivity of the mixture and the strong endothermic nature of carbon gasification may be the main determinants of the temperature gradients. Their results also indicated temperature gradients between 10 and 40°C/mm.

The main difference between this study and the studies mentioned above, are that none of the above studies investigated the effect of a continuously descending bed due to melting of the reduced or partially reduced product, while sustaining steady state solid-state reduction.

3.2 Determining rate constants for the reduction of iron ore

3.2.1 Solid state reduction kinetics

To eliminate unknowns during modelling of final reduction in the solids bed, representative rate constants for the reduction reactions (of the specific ore used during the investigation) had to be determined. The TGA experiment (discussed in ***paragraph 2.2***) was not designed to yield basic kinetic information and could therefore not be used for this purpose. Accordingly, data from a related study[51] was used to determine the kinetic rate constant for the reduction reactions. The original data from the experimental work was used to calculate the rate constants used in this paper.

The rate constants for the gasification reaction is calculated in a similar way than the reduction rate constant. For this study values recently measured for the specific coal that was used during this investigation, was used [51] .

3.2.1.1 Experimental aspects[51]

Experimental set-up

The experimental set-up consisted of a fluidised bed, which was mounted on a scale. This is schematically shown in ***Figure 30***. The scale enabled mass loss of the sample to be measured while the reactions occurred in the reactor. The reactor comprised of a double-shelled glass reactor. The inner glass reactor, which could be removed from the outer glass reactor, contained a perforated silica disc to allow gas flow from the outer glass reactor to the inner glass reactor. The perforated disc also ensured gas distribution through the sample.

The furnace temperature was controlled by a proportional-integral-derivative (PID) controller. A Pt/Pt10%Rh (or type S) thermocouple, positioned at the height of the sample, outside the outer glass reactor, served as control thermocouple. The outer reactor was mounted on the scale, which recorded mass loss as a function of time throughout each experimental run. Argon (99.999% purity) was used as purging gas, while CO (99.995% purity) was used as reduction gas, and CO_2 was used as oxidation gas. All of the gasses were passed through water vapour and oxygen removal columns (similar to that shown in ***Figure 13***) before introduction into the outer reactor. Gas flow rates were controlled by mass flow meters calibrated for each

specific gas. Flammable gasses CO and H_2 were burnt with a pilot flame at the gas outlet. The experimental set-up is discussed in more detail elsewhere[51].

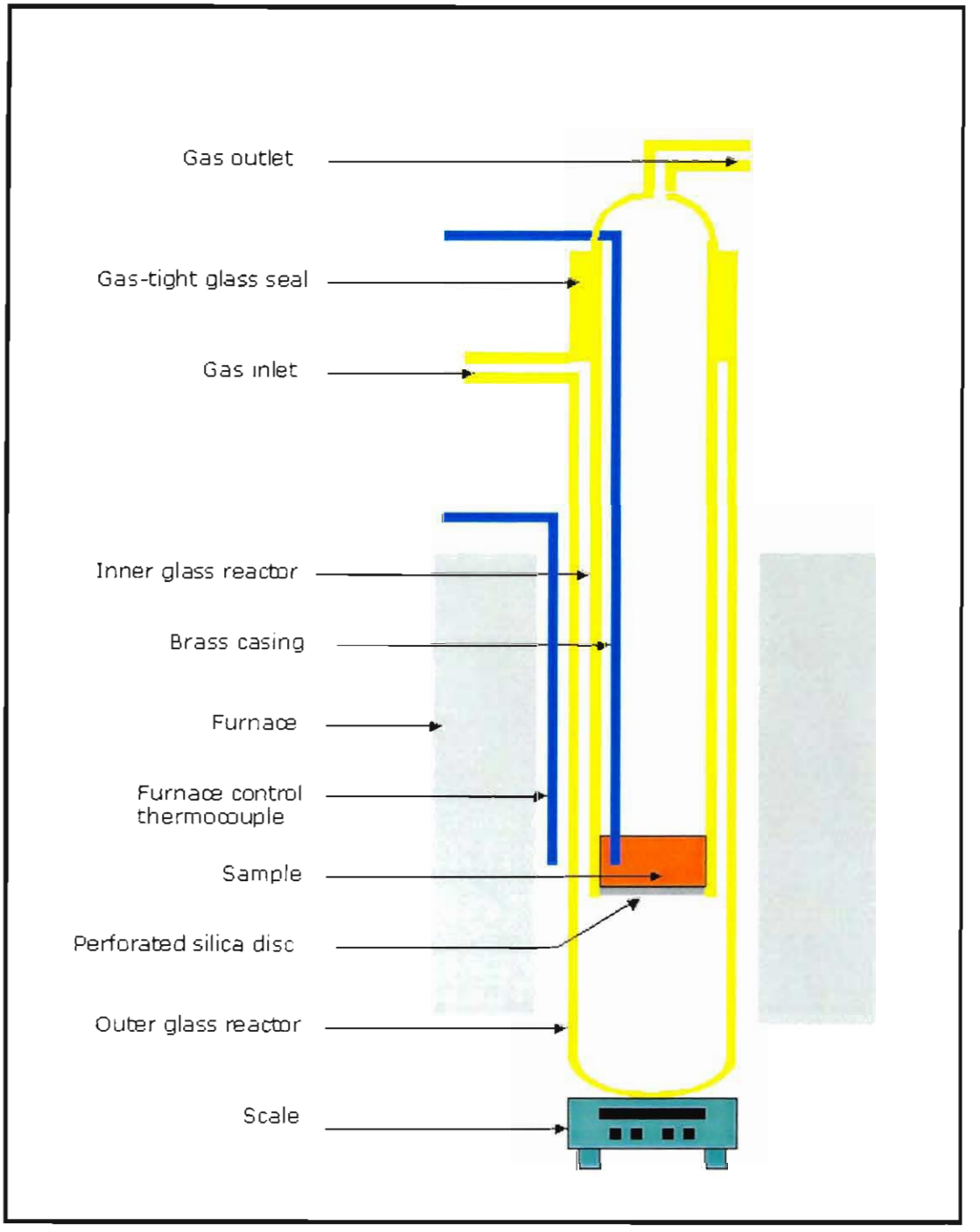

Figure 30: *Schematic presentation of the experimental set-up used for measuring rate constants*

Experimental Procedure[51]

Before the test commenced each sample was weighed. The sample was placed into the inner reactor, which was placed inside the outer reactor. The thermocouple was put in place to measure the sample temperature. The reactor was sealed and purging gas introduced. The mass recording software was activated and the mass of the sample was recorded continuously. The reactor was purged with Argon for 2 minutes, after which the Argon gas flow was terminated, and the reactant gas was introduced into the reactor at the required gas flow rate. The calculation of the required gas flow rate is shown in ***Appendix D.1***.

The sample was reacted for the required period. On completion of this period the reactant gas flow was terminated and the system was purged with Argon. After flushing for 5 minutes the inner reactor, containing the sample, was removed from the reactor assembly and allowed to cool to room temperature. Once the sample cooled to ambient temperature, it was recovered from the inner reactor, weighed, and analysed for degree of reduction.

For measuring of gasification reaction rates the same procedure was followed, but CO was substituted with CO_2. The experimental procedure is discussed in more detail elsewhere[51].

3.2.2 Results and discussion

A summary of the kinetic data from the reduction experiment with CO is shown in ***Table D.1*** to ***Table D.5*** and ***Figure D.2*** to ***Figure D.6*** in ***Appendix D.2.***

Reduction was assumed to proceed in the sequence hematite → magnetite → wustite → iron, with all reactions occurring as first order reactions. (Reduction of hematite to magnetite and magnetite to wustite was taken as one step.) The reaction rate of a first order reaction is described by the following relationship[51]:

$$\frac{dF}{dt} = -c\,(1-F) \qquad (3.a)$$

where *F* is the fraction of oxygen atoms reacted, t is the reaction time (with unit: s), and c is the proportionality constant (with unit: s^{-1}). Integration of ***equation 3.a*** between F and F_0, as well as t_0 and t yields the following equation:

$$\ln \frac{(1-F)}{(1-F_o)} = -c\,(t-t_o) \qquad (3.b)$$

From the experimental data, a plot of $\ln[(1-F)/(1-F_o)]$ vs $(t-t_o)$ was constructed. The slope of this plot yielded the proportionality constant c. This constant was expressed as follows[30]:

$$c = \frac{k_{co}\, m_{Fe}\, C_{co}}{N_0^O} \qquad (3.c)$$

where m_{Fe} was the mass of Fe in the sample (with unit: kg), C_{CO} was the concentration of CO gas in contact with the sample (with unit: mol/m^3) N_0^O was the initial oxygen content of the sample (with unit: mol), and k_{CO} was the rate constant (with units: $m^3.s^{-1}.kg\ Fe^{-1}$).

From ***equation 3.c***, the rate constant (k_{CO}) was calculated. The rate constant (k_{CO}) was expressed as follows:

$$k_{co} = k_o\, e^{(-E_a/RT)} \qquad (3.d)$$

where k_0 was the pre-exponential constant in rate expression (with units: $m^3.s^{-1}.kg\ Fe^{-1}$), E_a was the activation energy (with units: $J\ mol^{-1}$), R was the gas constant (with units: $J\ mol^{-1}\ K$), and T was the temperature (in K).

From a plot of $\log(k_{CO})$ vs 1/T, the value of the pre-exponential constant (k_0) and the activation energy (E_a) was obtained, by considering the intersect with the y-axis and the slope of the graph. Values obtained for the various size fractions of ore are presented in ***Appendix D.3***.

By plotting the ln of the rate constant against 1/temperature (the Arrhenius plot), the apparent activation energies as well as the k_o values of the reduction reaction for each particle size fraction of ore was determined. The Arrhenius plots are shown in ***Figure 31*** and ***Figure 32.***

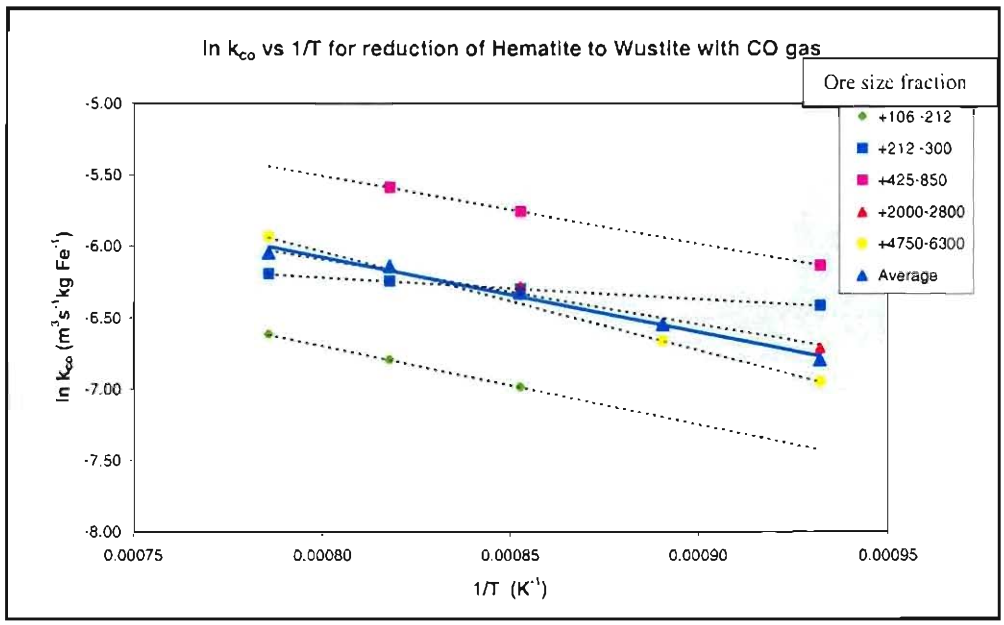

Figure 31: *ln (rate constants) as a function of 1/temperature for the reduction of hematite to wustite.*

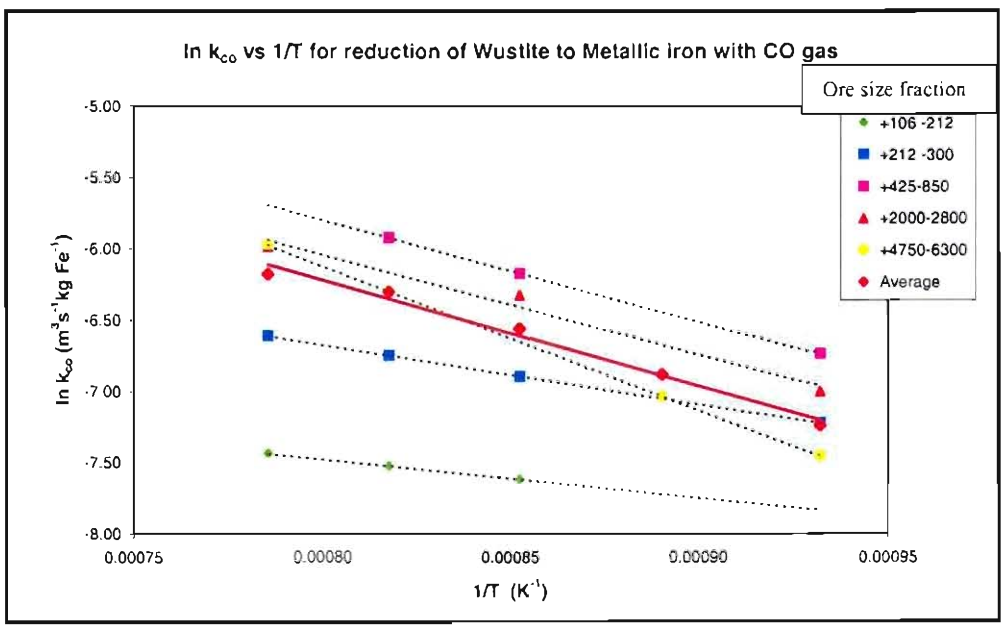

Figure 32: *ln (rate constants) as a function of 1/temperature for the reduction of wustite to metallic iron.*

Since the size distribution of the iron ore was known, the average rate constant and apparent activation energy was calculated from the weighted average plot of the plots for the individual size fractions. ***Figure 31*** and ***Figure 32*** (and ***Figure 33***) also shows the weighted average Arrhenius plot, which represents the plot for the ore fines with size distribution as used during this study.

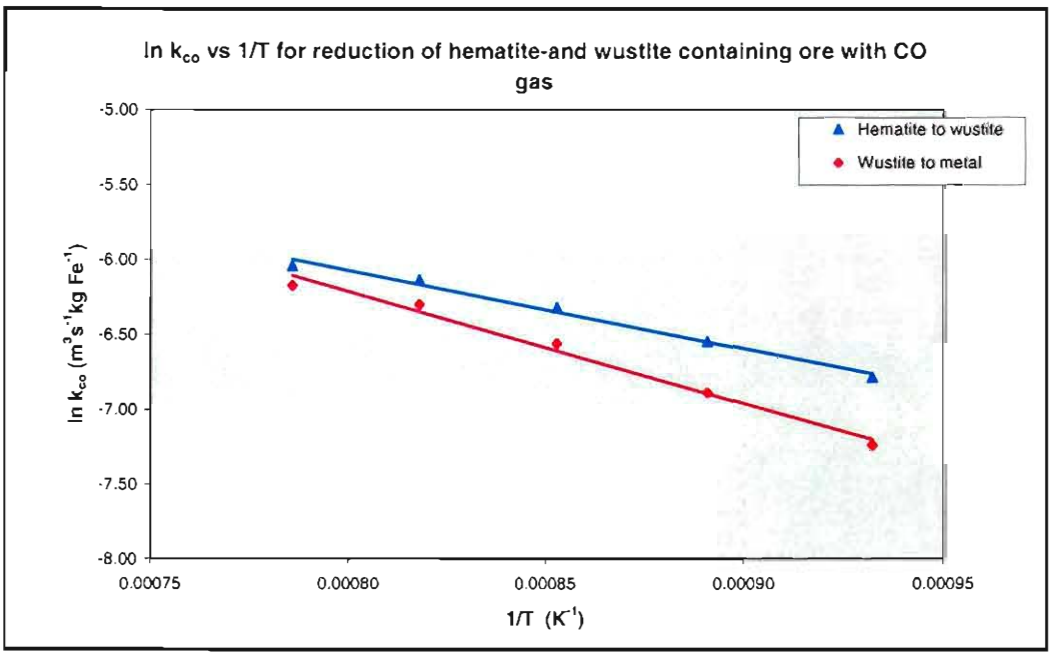

Figure 33: *Weighted averages of ln (rate constants) as a function of 1/temperature for the reduction of hematite to wustite and wustite to metallic iron respectively.*

The proportionality constants, rate constants and activation energies of the various particle sizes are shown ***Appendix D.3.*** The overall results are also shown in ***Table 5.***

Table 5: *Apparent activation energies and rate constants for Sishen ore used during this investigation.*

	0 to 30% reduction		30 to 80% reduction	
	k_o ($m^3s^{-1}kg\ Fe^{-1}$)	E_a ($J.mol^{-1}$)	k_o ($m^3s^{-1}kg\ Fe^{-1}$)	E_a ($J.mol^{-1}$)
Average values	0.535	56520	3.242	77000

The rate constants for the gasification reaction was measured by Pistorius et al[51] for char from the same Eikeboom coal that was used during this investigation. The rate constants for various size fractions of Eikeboom char was measured and the overall rate constant and activation energy was calculated. These values are shown in ***Table 6*** and ***Table 7*** respectively.

Table 6: *Individual activation energies and rate constants for gasification of specific size fractions of Eikeboom char, (which was also used during this investigation)*[51].

Size fraction of char	Carbon gasification	
	k_o ($m^3s^{-1}kg\ C^{-1}$)	E_a ($J.mol^{-1}$)
- 212µm +106 µm	4.588×10^4	182 440
-425µm + 212µm	1.252×10^4	166 769
-850µm + 425µm	6.180×10^2	137 098
-2000µm + 1400µm	8.255×10^4	189 867

Table 7: *Apparent activation energies and rate constants for gasification of Eikeboom char, which was used during this investigation*[51].

	Carbon gasification	
	k_o ($m^3s^{-1}kg\ C^{-1}$)	E_a ($J.mol^{-1}$)
Values used	45780	172401

3.3 Modelling of the bottom part of the solids bed

3.3.1 Basic model description[15]

3.3.1.1 Overview

The area in the solids bed where reduction mainly occurs by solid-state reduction, can be simulated as a plug flow reactor (PFR)[2]. On the other hand, the slag pool where solid/liquid state reduction and bath smelting reactions on be simulated as a continuous stirred tank reactor (CSTR)[2]. Based on the assumption that all material that reached the slag pool moved through the solids bed, final reduction at the bottom of the solids bed can be simulated as a PFR and CSTR in series. The relative amounts of reactions occurring in the PFR and CSTR depends on the respective amounts of solid-state reduction and solid-liquid-state reduction occurring in the process. This split in reduction mechanism was investigated during this study. The rate of reactions in the slag pool was assumed to be much faster than the rate of reactions in the solids bed[5,15].

The bottom of the solids bed was modeled as a PFR, using a kinetic model. The model was a variation of the model that was used by Pistorius[15] to simulate reduction in the top part of the solids bed. Since devolatilisation was expected to occur in the top part of the solids bed, volatiles were not included in the model. Although calcinations may or may not occur in the bottom part of the bed, the complexity of calcinations was excluded from the model. The solids bed therefore consisted of hematite, magnetite, wustite, metallic iron, carbon, and lime, while the gas phase comprised of CO and CO_2.

Since it was assumed that material moved through the solids bed in plug flow[15,16], one-dimensionality of the bed was assumed, i.e. properties varied only in the vertical direction.

The bed was divided into a number of horizontal cross-sections (or nodes). The condition in each node was assumed to be uniform. Coetsee et al.[49] showed that the gas temperature in a node could be assumed equal to the solids temperature in the node.

3.3.1.2 Thermal conductivity of the bed

The porosity of a nodes depended on the amounts of each of the phases present in the nodes, their densities and the node heights. The node height was assumed to remain constant during the reduction process. This means that compacting due to softening of the bed was not accounted for.

The effective thermal conductivity of each node was calculated using the geometric mean thermal conductivity of the solids[51], the conductivity of the gas[29], and the porosity of the node. This calculation was based on the assumption of random distribution of solids in each node (discussed in more detail in ***paragraph 2.3***).

3.3.1.3 Gas flow through the bed

The boundary condition at the bottom of the bed was a net flow of CO and CO_2 into the bottom node. The amount of CO and CO_2 corresponded to the amount of unreduced material leaving the bottom node. The CO/CO_2 ratio of this gas was chosen as 13, which corresponds with a partial oxygen pressure of $4x10^{-10}$, which in turn corresponds with a FeO activity of 0.3 at 1550°C. This correlates with pilot plant data[17].

The temperature of the gas entering each node was assumed to be equal to that of the solids in the node below it[49], while the gas leaves the node at the temperature of the solids in the node. For the bottom node the gas temperature was equal to the bath temperature.

The equilibrium partial pressures of CO_2 for the reduction and Boudouard reactions was calculated from equilibrium constants, which were derived from the free energy data as compiled by Kubaschewski et al.[53]

3.3.1.4 Reaction kinetics

Reduction was assumed to proceed in the sequence hematite → magnetite → wustite → iron, where the rate equation held for all three reduction steps. At temperatures below 564°C however, reduction was assumed to proceed in the sequence hematite → magnetite → iron, where the rate equation held for both reduction steps

The reaction rate expressions of the model were based on the expressions used by Coetsee et al.[30] during modeling of reduction of a composite pellet.

Reduction reaction:

$$r_R = k_R \exp(-E_R / RT)\, M_{Fe}\, (1-F)\, \frac{p_{CO} - p_{CO}^{R}}{RT} \qquad (3.e)$$

Boudouard reaction:

$$r_B = k_B \exp(-E_B / RT)\, M_C\, \frac{p_{CO_2} - p_{CO_2}^{B}}{RT} \qquad (3.f)$$

where r_R and r_B were the reaction rates (with units: moles of O and C reacted per m^2 per second), k_R and k_B were the rate constant for the reduction and Boudouard reactions respectively,(with units: m^3/kg Fe/s and m^3/kg C/s) , F was the degree of reduction achieved, M_{Fe} and M_C were the masses (in kg) of iron and carbon respectively per m^3 of the packed bed, E_R and E_B were the activation energies of the reduction and Boudouard reactions (with units J/mol), T was the absolute temperature, p_{CO} and p_{CO_2} were the partial pressures of CO and CO_2 respectively(with unit: Pa), p_{CO}^{R} and $p_{CO_2}^{B}$ were the equilibrium partial pressures of CO and CO_2 for the reduction and Boudouard reactions (in Pa).

3.3.1.5 Mass transfer and rate constants

Coetsee et al.[49] showed that the interface concentration of CO and CO_2, respectively was similar to the respective CO and CO_2 concentration of the bulk gas. Diffusion of gaseous species through the pores of the bed was therefore not considered in the model. The apparent rate constants (which makes provision for diffusion in the pores of the particle) were determined from experimental data, as discussed in ***paragraph 3.2***.

3.3.1.6 Calculation procedure

The initial conditions in the nodes was defined by the starting temperature, degree of reduction and the mass ratio of carbon and lime to iron.

The new temperature was explicitly calculated, and depended on the heat transfer into the node by radiation and conduction as well as the extent of reactions occurring

in each node. Radiation only took place at the bottom node, while the top node was assumed to be thermally insulated.

By considering an oxygen and carbon balance for each node, the CO/CO_2 ratio which satisfies the rate equations for the reduction and Boudouard reactions were found. The carbon and oxygen balances were written as follows:

Carbon balance: $n = (1 + x)(n_1 + n_2 + n_3)$ (3.g)

Oxygen balance: $n = (2 + x)(n_1 + 2n_2 + n_4)$ (3.h)

Where n_1 and n_2 were the amounts of CO and CO_2 , which respectively entered the node in a time interval (with units: mol/m^2), n_3 was the number of moles of carbon gasified by the Boudouard reaction (with units: mol/m^2), n_4 was the amounts of oxygen removed by the relevant reduction reaction (with units: mol/m^2), and x was the molar CO/CO_2 ratio of the gas leaving the node.

From ***equation 3.g*** and ***equation 3.h***, n_3 and n_4 were written as follows:

$$n_4 = C_1\left(p_{CO} - p_{CO}^{R}\right); \text{ with } C_1 = k_R \exp(-E_R / RT)\, M_{Fe}\, dh\, (1 - F)\, \frac{1}{RT}\, dt \quad (3.i)$$

$$n_3 = C_2\left(p_{CO_2} - p_{CO_2}^{B}\right); \text{ with } C_2 = k_B \exp(-E_B / RT)\, M_C\, dh\, \frac{1}{RT}\, dt \quad (3.j)$$

with dh the height of the node and dt the time interval (with unit: s) and all other symbols as defined for ***equation 3.e*** and ***equation 3.f***.

By combining ***equations 3.g*** and ***3.h***, and substitution of ***equations 3.i*** and ***3.j***, the following expression was obtained:

$$n_1 + 2n_2 + C_1\left(p_{CO} - p_{CO}^{R}\right) = \frac{x+2}{x+1}\left[n_1 + n_2 + C_2\left(p_{CO_2} - p_{CO_2}^{B}\right)\right] \quad (3.k)$$

In order to solve for X, ***equation 3.k*** was written in quadratic form as follows:

$$ax^2 + bx + c = 0 \tag{3.l}$$

with

$$\begin{aligned} a &= -n_2 - C_2 p^B_{CO_2} - C_1 p_{TOT} + C_1 p^R_{CO} \\ b &= n_1 - n_2 + C_2 p_{TOT} - 3C_2 p^B_{CO_2} - C_1 p_{TOT} + 2C_1 p^R_{CO} \\ c &= n_1 + 2C_2 p_{TOT} - 2C_2 p^B_{CO_2} + C_1 p^R_{CO} \end{aligned} \tag{3.m}$$

The quadratic equation was solved to yields a value for x, which was then used to solve for n_3, n_4 and n.

Once the amounts of Fe and C reacting was known for a time interval, an energy balance was performed to calculate the new temperature of the node, at the end of the time interval. The following equations were used:

$$T_{NEW} = (H_{INIT} + (q/A)_{cond\_in} + (q/A)_{Rad\_in} - (q/A)_{cond\_out} - SumA)/SumB \tag{3.n}$$

where T_{NEW} was the absolute new temperature of the node at the end of the time interval, H_{INIT} was the enthalpy of all species entering the node at the start of the time interval, $(q/A)_{cond\_in}$ $(q/A)_{Rad\_in}$ were the amounts of conductive and radiant heat (with units: J/m^2) which respectively entered the node during the time interval, while $(q/A)_{cond\_out}$ was the amount of conductive heat that left the node during the time interval.

$$H_{INIT} = \sum_i n_i \left(A_i + B_i T_{Node}\right) + n_1 \left(A_{CO} + B_{CO} T_{gas}\right) + n_2 \left(A_{CO_2} + B_{CO_2} T_{gas}\right) \tag{3.o}$$

$$SumA = \sum_j n_j \left(A_j\right) + xn\left(A_{CO}\right) + n\left(A_{CO_2}\right) \tag{3.p}$$

$$SumB = \sum_j n_j \left(B_j\right) + xn\left(B_{CO}\right) + n\left(B_{CO_2}\right) \tag{3.q}$$

where n_i is the number of moles of solid species *i* (Fe°, FeO, Fe_3O_4, Fe_2O_3, CaO and C) in the node at the start of the time interval, n_j was the number of moles of solid species j (Fe°, FeO, Fe_3O_4, Fe_2O_3, CaO and C) in the node at the end of the time interval, A_i , A_j, B_i and B_i are the constants in the enthalpy correlation[15] of species *I and j respectively*, n_1 and n_2 are the number of moles of CO and CO_2 respectively which entered the node, at the temperature T_{gas} , while *xn* and *n* were the number of moles of CO and CO_2 which left the node at the new temperature (T_{NEW}). Note that T_{gas} for node (n+1) was assumed equal to T_{Node} for node n.

This procedure was followed for all nodes in the solids bed, to yield the temperature profile of the bed at the end of time interval *dt.* The entire procedure was then repeated for various time intervals to find the change of temperature and degree of reduction with time.

3.3.1.7 Simulating feed rate:

To simulate feeding at the top of the solids bed with the simultaneous melting of the bottom of the bed, the solids bed moved down by a node thickness after a holding time which corresponded with the feed rate of iron ore. Feeding and melting therefore occurred as steps rather than continuous movement of the bed. After each step, the top node comprised of newly fed material , while the rest of the nodes each inherited the properties of the node above it (i.e. temperature, degree of reduction and carbon content).

This procedure was repeated until the change in temperature of the nodes became negligible. The temperatures of the nodes then showed the steady state temperature profile of the bed. Similarly, a reduction profile of the bed was found.

3.3.2 Model predictions

The predicted temperature profile as well as profile for degree of reduction through the solids bed, for a feed mixture containing 30% pre-reduced iron ore, is shown below:

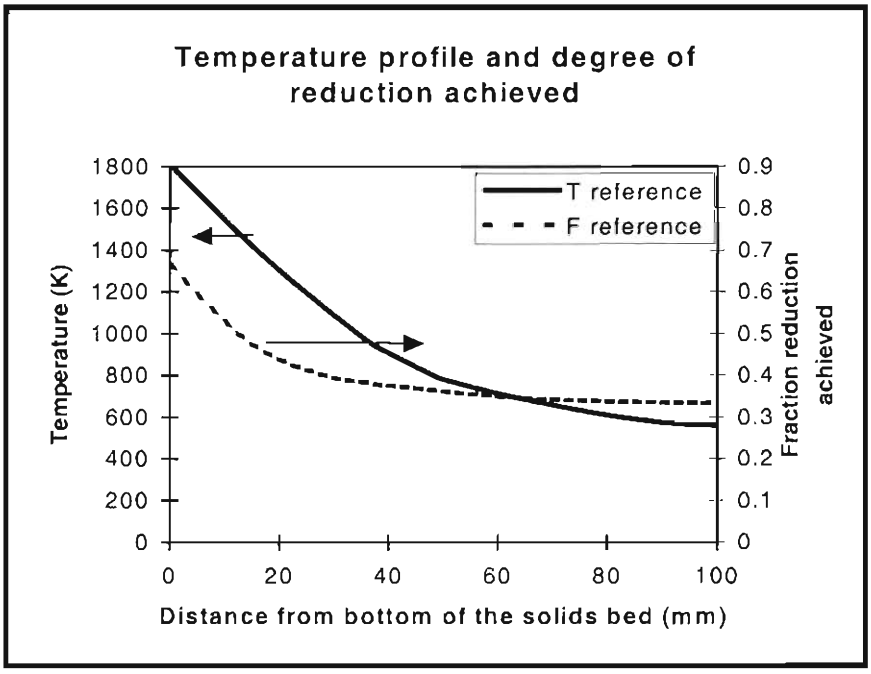

Figure 34: *Theoretical profiles of temperature and fraction reduction achieved through a 100mm high solids bed, for a production rate of 30kg/m²/h.*

Figure 34 shows that reduction mainly occurs in the 50mm above the bottom of the bed. These temperature and reduction profiles were used as basis for comparison when changes were made to the properties of the solids bed.

3.3.2.1 Change in rate constant for the reduction reaction

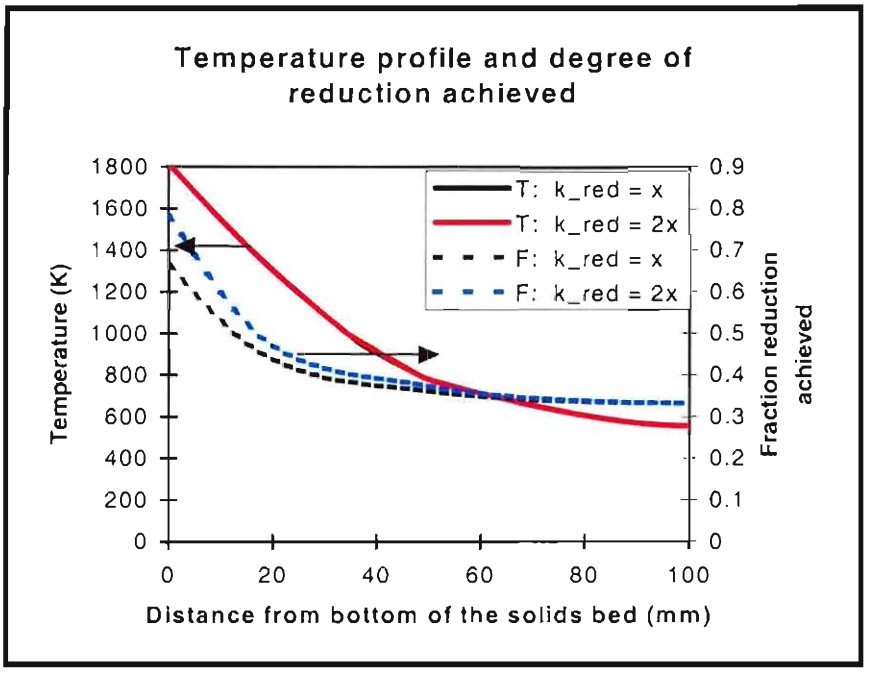

Figure 35: *Theoretical profiles of temperature and fraction reduction achieved through a 100mm high solids bed, for a production rate of 30kg/m²/h, when doubling the rate constant for the reduction reaction.*

Figure 35 shows the effect of doubling the rate constants for the reduction reactions on the profiles of the temperature and reduction achieved. The profiles for temperature and reduction for the increased rate constant are shown in red and blue respectively. The graphs presented in ***Figure 34*** are also shown as reference. The figure clearly indicates that the reduction profile changes. Before the rate constant was changed, 66% reduction was theoretically achieved, while 78% reduction was achieved when the rate constant was doubled. The temperature profile of the bed was not affected by the change in rate constants (the solid red and black lines were exactly the same).

From the above it seems that the degree of reduction achieved is controlled by the rate of the reduction reaction. Accuracy regarding the reduction rate constant (discussed in ***Section3.2***) used during modelling of the solids bed is therefore important.

Figure E 2 in ***Appendix E.1*** shows the theoretical profiles of temperature and fraction reduction through a 100mm high solids bed, for a production rate of 30kg/m^2/h, when the rate constant for the reduction reaction is halved. The effect thereof was that 8% less reduction was achieved, while the temperature profile of the bed was unchanged.

3.3.2.2 Change in rate constant for the gasification reaction

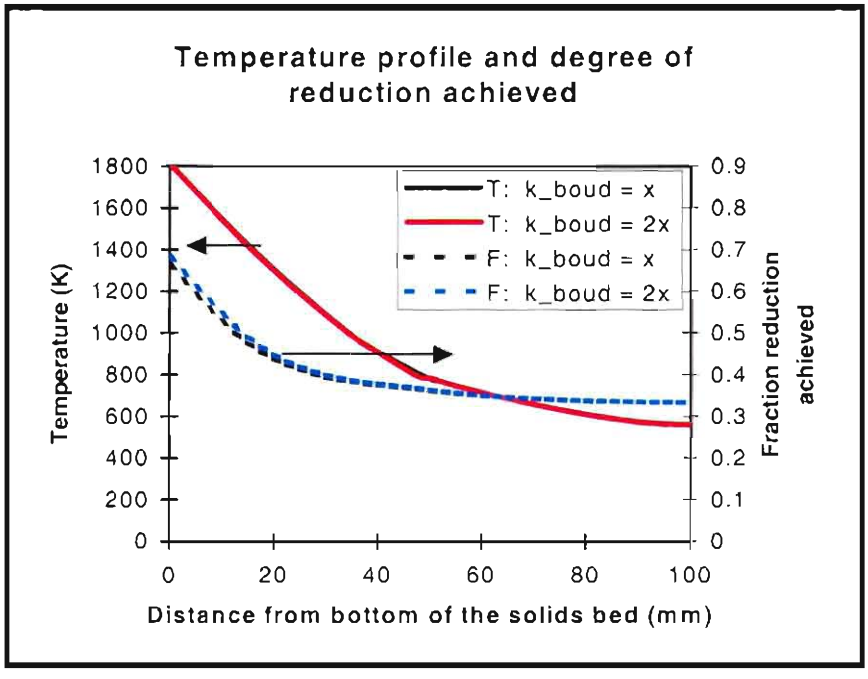

Figure 36: *Theoretical profiles of temperature and fraction reduction achieved through a 100mm high solids bed, for a production rate of 30kg/m^2/h, when increasing the rate constant for the gasification reaction.*

Figure 36 shows the effect of doubling the rate constants, for the gasification reactions, on the temperature and reduction profiles. The profiles for temperature and reduction are shown in red and blue respectively, while the results from ***Figure 34*** are also shown in black. The figure indicates that neither the temperature nor the reduction profiles changed significantly when the gasification rate constant was doubled. This implies that the rate of reduction at the bottom of the solids bed is not governed by the chemical rate of the Boudouard reaction.

Since it appeared that the rate of reduction was not controlled by the rate of the gasification reaction as such, accuracy regarding the rate constant for the gasification reaction was not regarded critical for modelling purposes.

Figure E 4 in ***Appendix E.1*** shows the theoretical profiles of temperature and reduction achieved through a 100mm high solids bed, when the rate constant for the Boudouard reaction is halved. Changing of the gasification rate constant did not change the temperature profile or the reduction profile of the bed.

3.3.2.3 Change in thermal conductivity of the bed

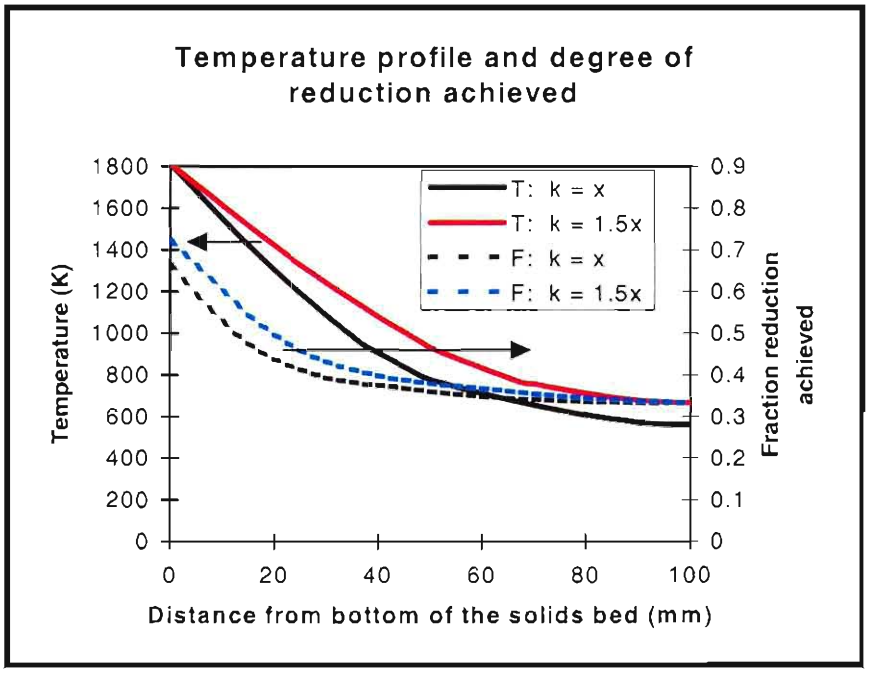

Figure 37: *Theoretical profiles of temperature and fraction reduction achieved through a 100mm high solids bed, for a production rate of 30kg/m^2/h, when increasing the thermal conductivity of the solids bed 1.5 times.*

Figure 37 shows the effect of increasing the thermal conductivity of the solids bed by a factor of 1.5. The figure shows a significant decrease in the slope of the temperature profile (in red) as well as a 7% increase in the degree of reduction achieved (in blue).

From the above it is clear that the overall reduction rate is not only controlled by the rate of the reduction reaction (as discussed in 3.2.2.1) but also by the rate of heat transfer (via conduction) in the solids bed.

Figure E 6 in ***Appendix E.1*** shows that halving of the thermal conductivity resulted in about 10 % less reduction achieved, while the slope of the temperature profile increased .

3.3.2.4 Change in bath temperature

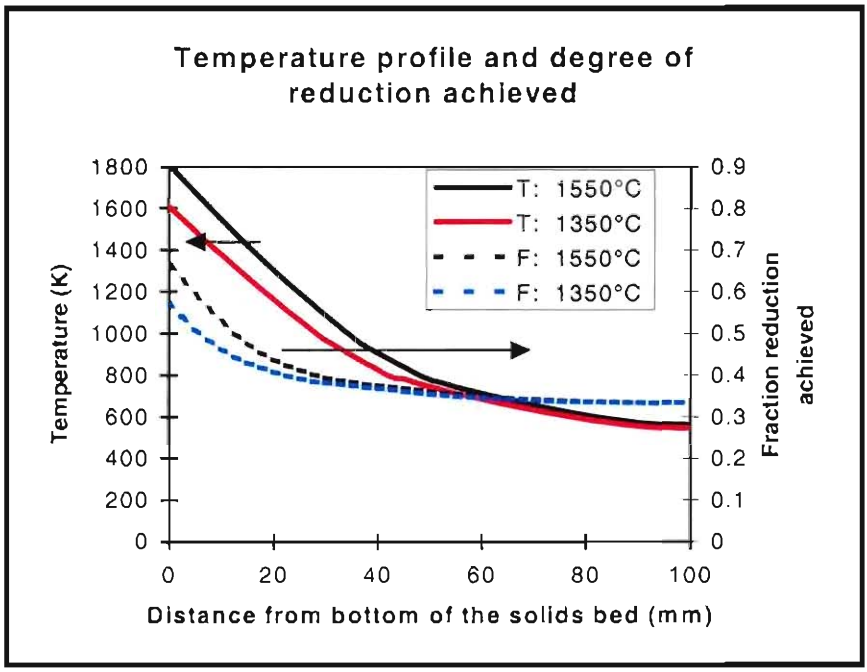

Figure 38: *Theoretical profiles of temperature and fraction reduction achieved through a 100mm high solids bed, for a production rate of 30kg/m²/h, when decreasing the bath temperature.*

Figure 38 shows the effect of decreasing the bath temperature from 1550°C to 1350°C. The figure shows a temperature profile (in red) at a lower position but with similar slope than that of **Figure 34** (shown in black). The reduction profile (shown in blue) also changed with a decrease in bath temperature. This indicated the importance of maintaining a constant bath temperature for comparative purposes.

Figure E 7 in ***Appendix E.1*** showed that when the bath temperature was increased from 1550°C to 1750°C, a larger temperature gradient and a higher degree of reduction was achieved.

3.3.2.5 Change in production rate

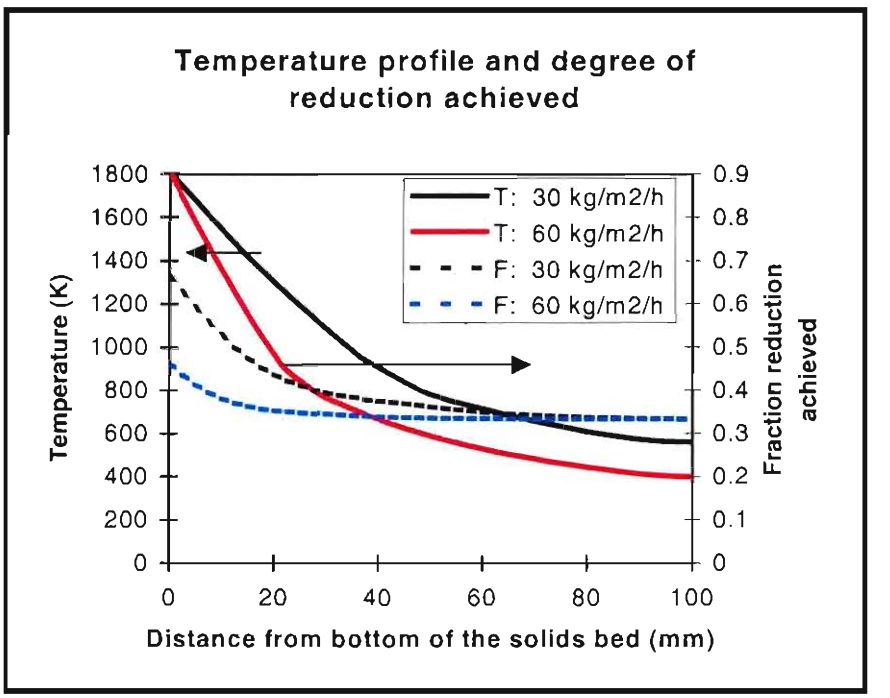

Figure 39: *Theoretical profiles of temperature and fraction reduction achieved through a 100mm high solids bed, for a production rate of 30kg/m^2/h as well as 60kg/m^2/h.*

Figure 39 shows the effect of increasing the production rate from 30 kg/m^2/h to 60kg/m^2/h. The figure shows a significant increase in the slope of the temperature profile, and accordingly, lower temperatures (in red). The figure also shows a significant decrease (about 20%) in the degree of reduction achieved (in blue). This indicated that the degree of reduction achieved in the solids bed strongly depended on the residence time of the particles in the solids bed.

Figure E 10 in ***Appendix E.1*** shows that when the production rate was halved, the degree of reduction achieved increased by about 20%, while the slope of the temperature profile of the bed decreased.

3.3.2.6 Change in degree of pre-reduction of input material

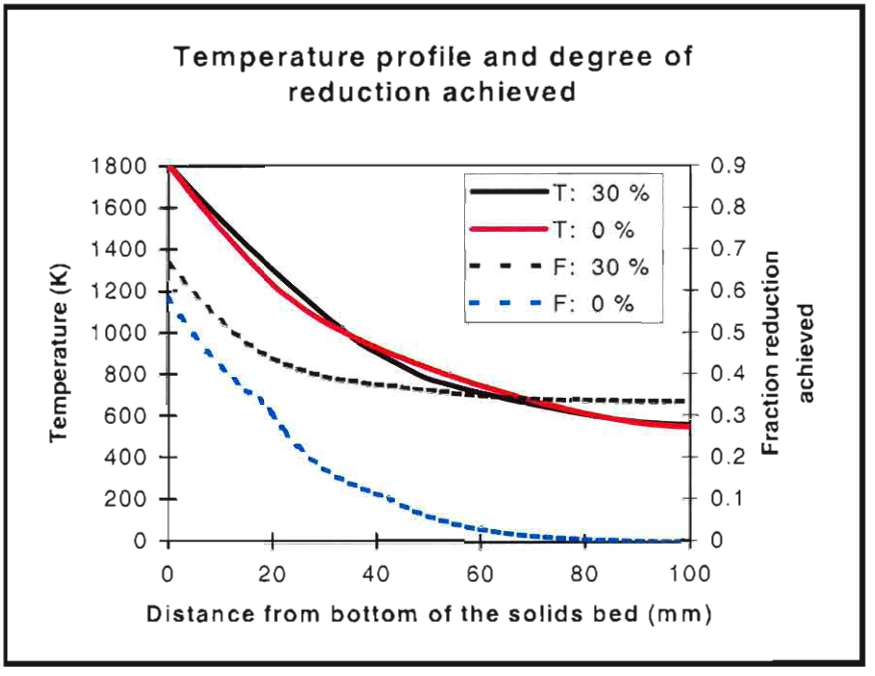

Figure 40: *Theoretical profiles of temperature and fraction reduction achieved through a 100mm high solids bed, for a production rate of 30kg/m²/h when decreasing the degree of pre-reduction of the input material from 30% to 0%*

Figure 40 shows the effect of decreasing the extent of reduction achieved in the upper part of the solids bed (from 30% to 0%). The figure shows little change in the slope of the temperature profile (in red), while the final degree of reduction achieved at the bottom of the solids bed (in blue) decreased (from 66% to 59% reduction).

Figure 41 shows the effect of increasing the extent of reduction achieved in the upper part of the solids bed from 30% to 50%. The figure shows that the slope of the temperature profile decreased, while the final degree of reduction achieved at the bottom of the solids bed (in blue) increased with 10%..

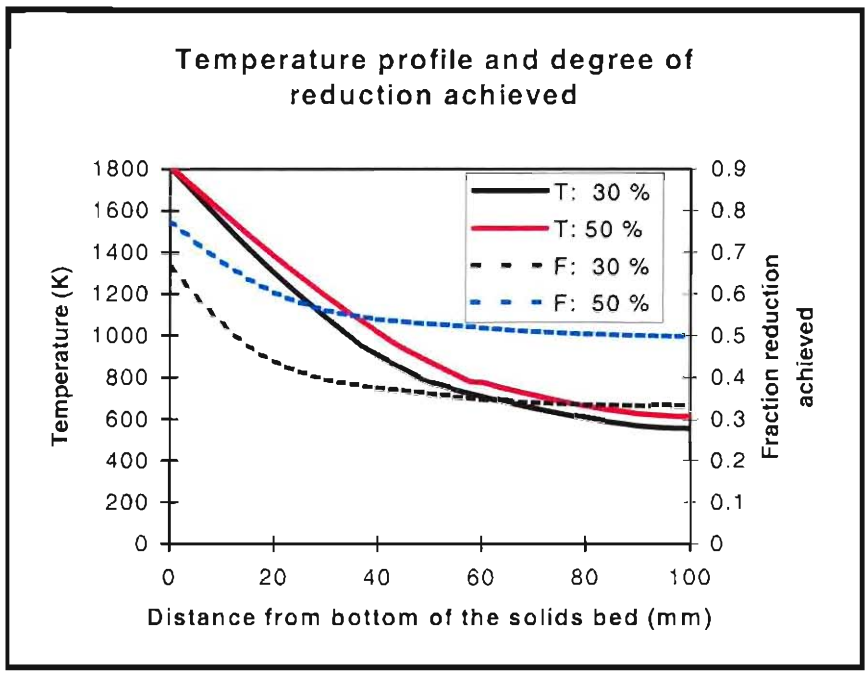

Figure 41: *Theoretical profiles of temperature and fraction reduction achieved through a 100mm high solids bed, for a production rate of 30kg/m^2/h when increasing the degree of pre-reduction of the input material from 30% to 50%*

The next step was to measure these model predictions experimentally.

3.4 Experimental aspects

3.4.1 Experimental apparatus

The experimental equipment mainly comprised of the induction furnace and associated gas flow rate control system.

3.4.1.1 The induction furnace setup.

The tests were performed in a 150kW coreless induction furnace. The furnace consisted of a fixed water-cooled induction coil, a fixed refractory lining, a removable crucible and a crucible lid assembly (shown in ***Figure 42***)

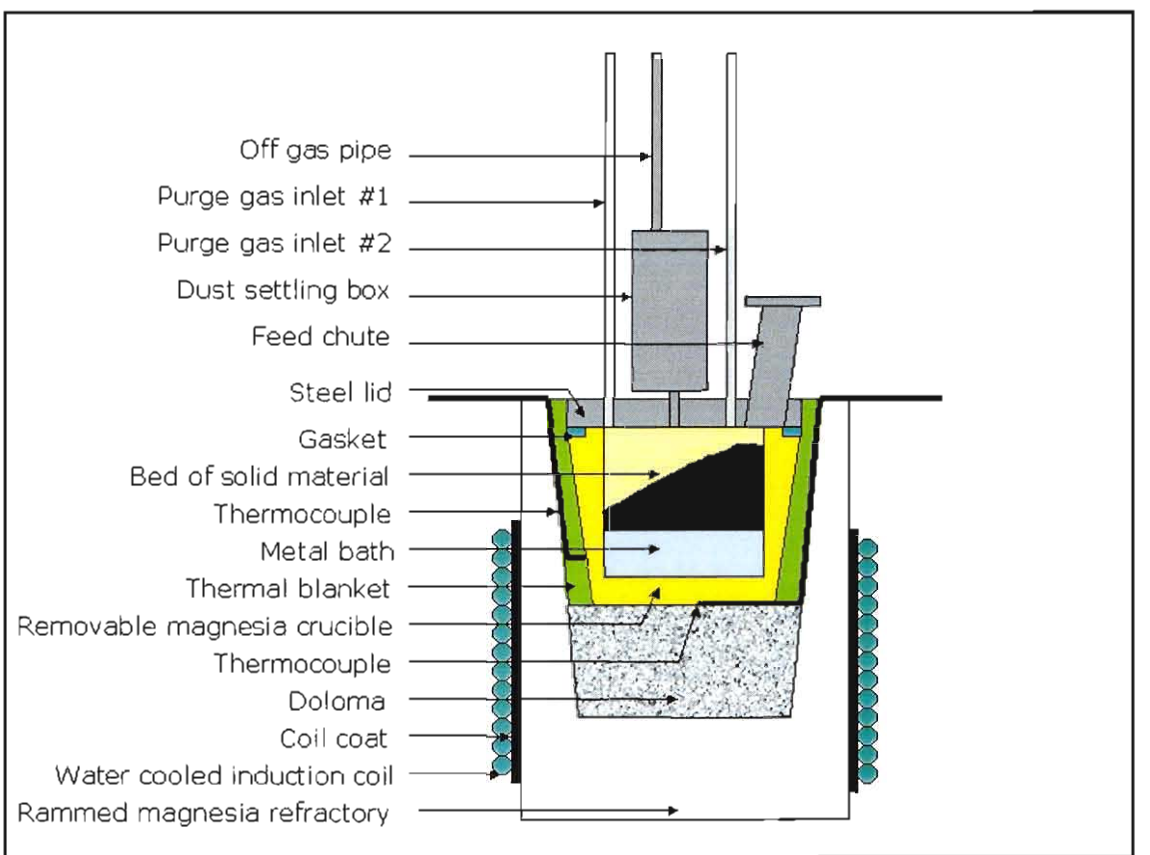

Figure 42: *Schematic illustration of the induction furnace configuration.*

The furnace was heated with a water-cooled, copper induction coil of 340 mm inside and 400 mm outside diameter, with a height of 465 mm. The coil was covered with high temperature insolating paper, to serve as coil coating. Since the furnace refractories expand and contract during heating cycles, the coil had to be separated

from the furnace refractories. This enabled stable coil conditions, despite expansion and contraction of furnace refractories.

The walls of the furnace were rammed, using a high magnesia ramming material (Basiram 95 HK) from Hernic Premier Refractories. Prior to test work, the rammed lining was sintered by establishing, and maintaining a steel bath in the furnace for three hours. The furnace was tapped (by tilting), and after cooling the metal scull was removed.

The floor of the furnace was lined with a layer of doloma (burnt dolomite) of particle size between 2.8 mm and 3.3 mm diameter. This was done to avoid "sticking" of the magnesia crucible to the magnesia furnace refractories (due to sintering), thereby easing removal of the "removable crucible".

The removable crucible was positioned on top of the doloma. (The positioning of the crucible is discussed in more detail in ***Appendix F.2***.) Each crucible had a 160 mm inner diameter and a height between 235 mm and 240 mm, while the outer diameter tapered from 190 mm to ±215 mm. The crucibles were cast with Basiram 95 HK from Hernic Premier Refractories. The water addition needed to obtain the castable was 7% (as specified by the manufacturers). The crucibles were cast in plastic moulds, and dried at 110°C for 36 hours. The crucibles were freed from the mould by breaking (cutting and tearing) the moulds. Sintering of the crucibles was done in a muffle furnace, with temperature control by PID (proportional integral derivative) controller. The sintering cycle comprised of heating from ambient to 1500°C over a period of 60 hours and cooling to ambient over another period of 60 hours.

In the experimental set-up, the crucible was covered with a steel lid. The off gas pipe extended through the steel lid. A gasket, cut from a high alumina thermal blanket (1400°C grade) was placed between the crucible and the lid. Since the steel lid was held in position by its own weight, and could be lifted by pressure inside the crucible (the entire lid acted as an pressure relieve damper) the crucible arrangement could not be made gas tight. A positive pressure was therefore maintained in the crucible to prevent air from leaking into the crucible. This was done by purging the crucible with argon.

The feed system of the furnace consisted of a feed chute, onto which a removable glass lid was fastened with clamps. A rubber packing ensured a gas-tight seal between the glass lid and the chute. The chute extended through the crucible lid, into the crucible.

A 4 mm hole through the crucible lid enabled access of thermocouples to the inside of the crucible, for measuring the temperature profile of the solids bed.

The cavity between the removable crucible and the furnace refractories was filled with an alumina fibre thermal blanket. This improved thermal insulation of the crucible and also served to hold the thermocouples in position.

3.4.1.2 Gas system

The crucible assembly was continuously purged with 99.999% pure Argon. A schematic diagram of the gas preparation and control system is shown in ***Figure 43***. The respective gas lines, their purification trains, connecting gas-lines and stopcocks are indicated.

A ball valve was used to set the flow rate of the purge gas. The argon passed through a hydrosorb cartridge (from Messer Griesheim) to remove traces of moisture. According to specifications the final purity of the gas was < 0.5 ppm H_2O.

To avoid oxidation of the sample (and product gas from the sample) the oxygen potential of the purge gas was regulated. This was done by passing the argon through oxisorb-W (also from Messer Griesheim), which comprises activated chromium trioxide that absorbs traces of oxygen in the gas. According to specifications, the oxygen content of the gas is lowered to below 10ppb (which corresponds to an oxygen potential below 10^{-8} atm). Changes in colour indicated when the cartridges needed replacement.

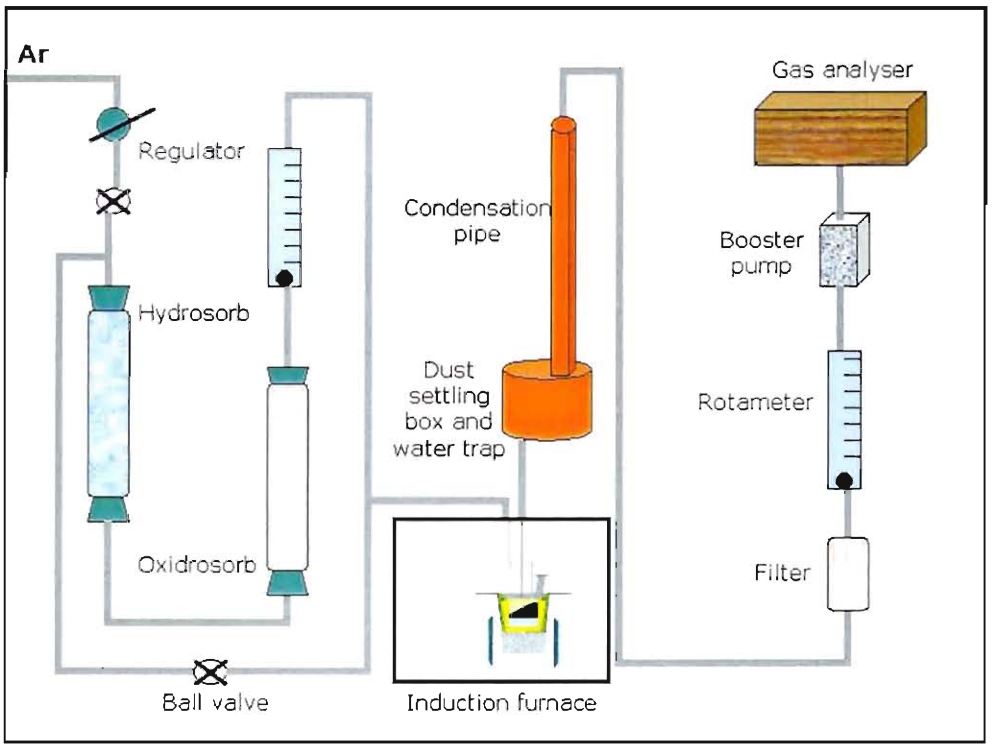

Figure 43: *Schematic illustration of the gas system configuration.*

The flow rate of the Argon was measured with a calibrated rotameter from Fisher Porter (model 10P6132NA). Calibration of flow meters is discussed in ***Appendix F.3***. From the rotameter, the gas line split into two gas supply lines, both leading directly to the crucible lid, for flushing. (Two supply lines were used for the argon in an attempt to induce mixing of the purge gas with the CO and CO_2 that evolves from the solids bed.) Purge gas entered the crucible, through two copper tubes that extended through the crucible lid. Off-gas exited the furnace through a steel tube, which also passed through the lid.

Since the gas analyser needed a gas flow rate of 6 l/min to operate accurately, at least 6 litres of gas had to be either produced inside, or blown into, the crucible. To avoid air from entering the crucible, the crucible was operated with a slight positive pressure. For this, the flow rate of argon into the crucible, was maintained at 6 l/min. The product gas from the reactions in the crucible then resulted in a positive pressure inside the crucible.

The off gas from the crucible passed through a dust-settling box of about 5 dm^3, made from mild steel. From the box, the gas passed through a steel cooling pipe of 25 mm diameter and 1 m long. This was intended to allow water vapour to condense and drip into the dust-settling box. The gas then passed through a Balston (model 9556-1/4) filter, with replaceable filter elements. These filter elements were replaced after each test.

The gas was passed through a calibrated rotameter, from where it went through a booster pump, to the gas analyser. A Prima 600 mass spectrometer was used for analysing of the gas.

3.4.2 Experimental procedure.

3.4.2.1 Raw material preparation

The ore, coal and fluxes used during this investigation were similar to those used for the reference sample for the TGA tests (the first phase of the investigation).

Dolomite and limestone samples were compiled according to the size distributions in ***Table A 2*** in ***Appendix A.3*** To avoid complications associated with the calcinations reactions, calcinated dolomite (doloma) and calcinated limestone (lime) were used. For calcination, the dolomite and limestone were placed in alumina crucibles and exposed to 1000°C for a period of 16 hours (overnight) in a muffle furnace.

Since devolatilization is expected to occur in the upper part of the solids bed, coal char was used in the mixture. The coal was charred at 1000°C. This was done by heating 7 kg batches of coal, at such a rate that 1% mass loss occurred every 10 minutes. The coal was charred until no further mass loss occurred. Charring was done in a nitrogen atmosphere. After cooling, the char was screened and samples were compiled so that the size distribution of each sample matched the size distribution of the coal in ***Table A 2*** in ***Appendix A.3.***

The ore samples were all synthetically compiled to match the size distribution of ore in ***Table A 2*** in ***Appendix A.3***. Three series of ore samples were prepared for testing.

The first sample series comprised of unreduced hematite ore.

The second series comprised of iron ore that was 30% pre-reduced at 800°C. For this a thermo gravimetric analyser (TGA), with a capacity of 7kg, at Kumba's technology department was used. A gas flow rate of 1 l/min was maintained to avoid fluidisation of the material, and a reducing gas comprising 50% CO and 50% CO_2.was used. (The temperature and gas composition was chosen so that the stable phase that formed would be wustite)[7]. The mass of the sample was registered continuously, as indication of the degree of reduction achieved.

The third series was 50% pre-reduced at 1000°C, using a gas containing CO and CO_2 in a 2:1 ratio, so that the stable phase that formed would be metallic iron[7].

The char content of the samples were chosen so that the material mixture comprised a $FC/O_{(ore)}$ ratio of 0.85. The selection of a $FC/O_{(ore)}$ ratio of 0.85 is discussed in more detail in ***Appendix F.1.***

3.4.2.2 Test Procedure

Prior to testing the mass of the removable crucible as well as the mass of the metal (to be melted as metal bath) recorded. The experimental configuration, as described previously, was assembled. A metal bath was established by melting two metal discs of 150mm diameter and weighing about 12kg in the removable crucible, in the induction furnace (see ***Figure 44***). The scrap metal used was cut from the same sheet of grade 300 WA steel, produced at Highveld Steel and Vanadium Corporation Ltd. The certified analysis of the steel is shown in ***Table 8***

Table 8: *Analyses of 300 WA sheet steel used to establish the metal bath.*

	C (%)	S (%)	P (%)	Si (%)	Mn (%)	Cr (%)	Vl (%)
300 WA	0.17	0.02	0.005	0.26	0.91	0.05	0.01

During heating of the discs, the temperatures of the discs and outer surface of the crucible (at the bottom and on the sidewall) were recorded. The power input to the furnace was regulated so that a heating rate of ±300°C/hour was achieved.

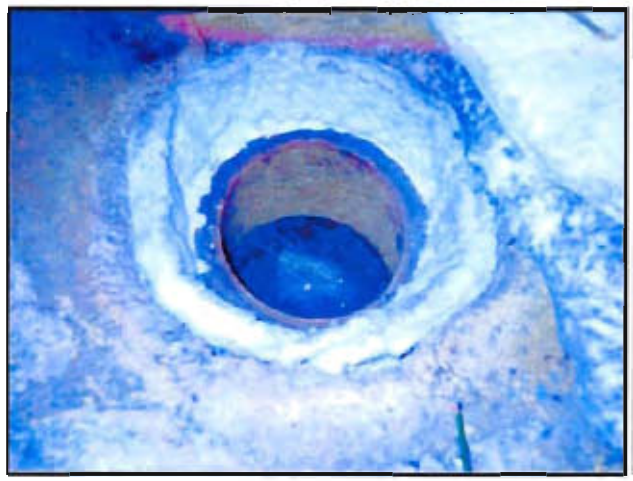

Figure 44: *Crucible with scrap for metal heel in induction furnace.*

Figure 45: *Establishing of a solids bed on top of the molten bath.*

As soon as the discs melted, and a liquid bath was established, ± 1kg of feed mixture was fed onto the liquid bath. This is shown in ***Figure 45***. The lid of the crucible was then positioned on top of the crucible, and the argon gas flow was established to flush the crucible, and establish a positive pressure inside the crucible. An additional ±500 g of feed mixture was fed into the crucible, to establish a solids bed (as a pile) with apex about 2 to 5 cm below the crucible lid. Batches of material mixture (±250g) were then fed onto the solids bed, at such intervals to maintain a constant bed height. Access to the crucible was obtained by a feed chute that extended through the crucible lid. During operation the chute was closed with a removable glass lid, which clamped onto the end flange of the chute. For gas tightness a rubber gasket was placed between the glass lid and the end flange of the chute. This configuration is shown in ***Figure 46.***

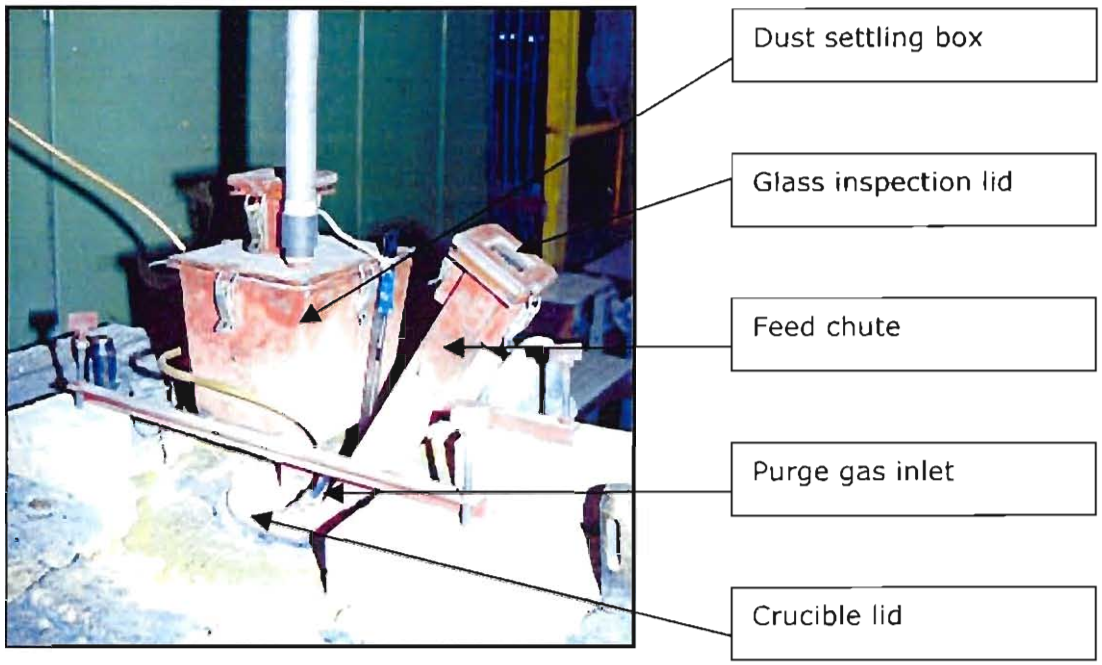

Figure 46: *Lid with feed chute on top of crucible.*

The production rate was estimated from the rate at which material had to be fed to the furnace to maintain constant heap heights, as well as from gas analyses.

A multi-channel Prima 600S gas analyser was used to analyse the off gas. Off gas from the crucible (comprising of product gas and purge gas) was pumped to a gas analyser at a rate of 6 l/min. This is the minimum gas flow rate specified for the gas analyser. Analyses were performed at approximately two-minute intervals, depending on the amount of channels in use during an experiment.

Since the rate at which argon was blown into the "freeboard" of the crucible was known, the rate at which CO and CO_2 entered the "freeboard" of the crucible was calculated from the off gas analyses. (The CO to argon flow ratio in the off-gas is directly shown by the off-gas analysis, when perfect mixing is achieved in the "freeboard" of the crucible.) The rate at which CO and CO_2 leaves the crucible translates to the rate at which oxygen is removed from the crucible and therefore gives the rate of reduction (and metal production) in the crucible

Excess process gas that escaped from the system, were extracted through the roof extractor fans. For safety reasons the CO content of the furnace surroundings were continuously monitored, using a Dräger CO monitor.

The power input to the furnace was manually regulated in an attempt to achieve the desired production rate. Although mass and energy balance calculations showed that approximately 4 kW power input was needed to drive the reduction and melting reactions, about 40 kW power input was needed to prevent solidification of the bath. Accordingly, an estimated 90% of the power input was used to overcome heat losses. The amount of heat losses however varied from one experiment to the next, thereby complicating control of the electrical power input for the process. The capacitor arrangement of the furnace also had to be changed intermittently, to ensure operation with a phase angle close to zero. (A zero degrees phase angle translates to a power factor of one, which indicates optimum utilisation of power).

The temperature on the outer surface of the crucible was measured continuously during each test. This was done to avoid overheating of the metal bath.

Once at least 3 kg of material was fed to the furnace, the temperature profile of the solids bed was measured. This means that the temperature profile was only measured once the furnace was operated for a period longer than the residence time of material in the solids bed (to achieve steady state operation in the furnace). The temperature profile is the variation of temperature with vertical position in the bed. During initial tests, chromel(Ni-Cr)/alumel(Ni-Al) (or type K) thermocouples were used, but during the last series of test, Pt/Pt10%Rh (or type S) thermocouples were used. The reference height for measurements was the height of the crucible lid. The profile was measured by pushing a thermocouple vertically down, (through a 4 mm hole in the crucible lid) into the bed. The thermocouple temperature and the distance by which the thermocouple was lowered into the bed were recorded simultaneously. The thermocouple was lowered 5 mm at a time, and held in position until the measured temperature approached a constant value.

The height of the metal bath was measured by inserting a 3 mm mild steel rod 300 mm deep into the crucible, through the hole that was used for measuring the temperature profile. Upon extrusion of the rod, the height of the metal bath (relative to the height of the lid) could be seen. This is similar to the "dip rod" method used

to determine the bath level in pilot plant furnaces. Note further that the temperature profile was also measured relative to the height of the lid. With these measurements the temperature profile of the solids bed was expressed relative to the height of the bottom of the solids bed.

After the temperature profile of the heap was measured, the temperature of the metal bath was also measured. For this a Pt/Pt10%Rh (or type S) thermocouple, shielded in a Metamic 829 sheath was used. These types of sheaths comprise 70 % molybdenum and 30 % alumina, and are normally used in vacuum melting furnaces.

At the end of the experiment, the crucible was lifted from the induction furnace and left to cool to ambient temperature, as shown in ***Figure 47***. A custom made, pliers-like, tool was used for lifting and transporting of the hot crucible.

Figure 47: *Crucible removed from the furnace for cooling.*

After cooling, the mass of the crucible with its content was weighed. The loose material in the crucible was poured out of the crucible, and the material remaining in the crucible was impregnated with cold-setting Araldite M Resin containing 20% Araldite HY 956 hardener. Once solidified, the refractory was removed from the sample (with a hammer and chisel) and the sample was cut in vertical slices, to reveal a picture of the bottom of the solids bed. Some of the samples were polished to a mirror-like finish. Final polishing was done with 3µm diamond paste. Typical images obtained are shown in ***Appendix F.***

3.4.2.3 Temperature control of the liquid bath

The method used to monitor changes in the bath temperature was based on a method used by Duca[54], who measured the refractory temperature to determine the extent of wear of the induction furnace refractories.

The furnace temperature was regulated manually according to the change in temperature of the outer surface of the removable crucible. Three Pt/Pt10%Rh (or type S) thermocouples were installed to measure the temperature on the outer surface of the crucible. Two of these were placed along the sides of the crucible, at the height of the metal bath, while the third was placed, in the centre, below the crucible. The thermocouples were made of 0.38 mm diameter thermocouple wire, which was certified to be accurate within one degree, by the suppliers, Johnson & Matthey.

A combination of an "Adams 4017 data acquisition module" and an "Adams 4520 RS 232 to RS 422 / RS 485 converter" was used to convert the milli-volt output, of the thermocouple to a RS 232 digital signal. This signal was recorded with custom made software, and exported to an excel spreadsheet. The data acquisition and recording equipment is shown in ***Figure 48***.

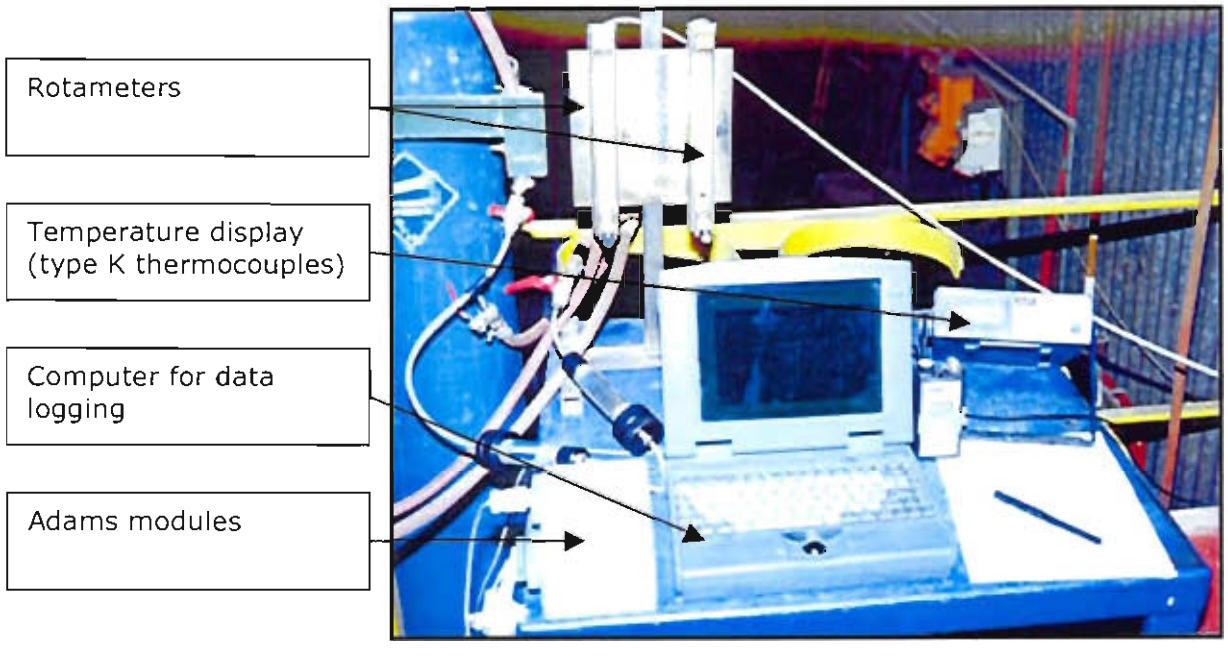

Figure 48: *The data acquisition and recording equipment*

Variations of the temperatures of the outer surface of the crucible, reflected variations of the bath temperature. This means that when the temperature of the bath increased, the recorded temperature also increased, and vice versa. At the start of each test, the bath temperature was directly measured using a sleeved Pt/Pt10%Rh (or type S) thermocouple. The directly measured bath temperature was used as a reference for the temperature measurements on the outer surface of the crucible.

3.4.3 Results and discussion

3.4.3.1 Bridging of solids bed

From time to time, the solids bed stuck to the walls of the crucible, thereby forming a "bridge" in the crucible. This resulted in heat from the metal bath being transferred by radiation to the bottom of the solids bed. The model was accordingly changed to simulate this condition. (The gap that formed between the solids bed and liquid bath is seen in the visual sections of the solids bed, shown in ***Appendix F***)

Bridging of the solids bed also resulted in poor control regarding the production rate. When the energy input to the furnace was increased, the bath temperature increased, which resulted in an increase in production rate. Changing the production rate, while maintaining a constant bath temperature was therefore problematic. The approach with the experiment therefore changed from regulating the production rate to measuring the production rate, in order to obtain data that could be compared to model predictions.

3.4.3.2 Production rates

From the gas analyses (presented in ***Appendix F.5***), the production rates were calculated. Results are presented in ***Figure 49***, ***Figure 50*** and ***Figure 51***.

Sudden increases in the production rate were recorded from time to time. This was due to unsteady operations when too much energy was supplied to the bath, resulting in intermitted moments during which high production rates were observed. In order to achieve stable (near steady state)conditions, production rates in the region of 20 kg Fe/m^2/h had to be maintained

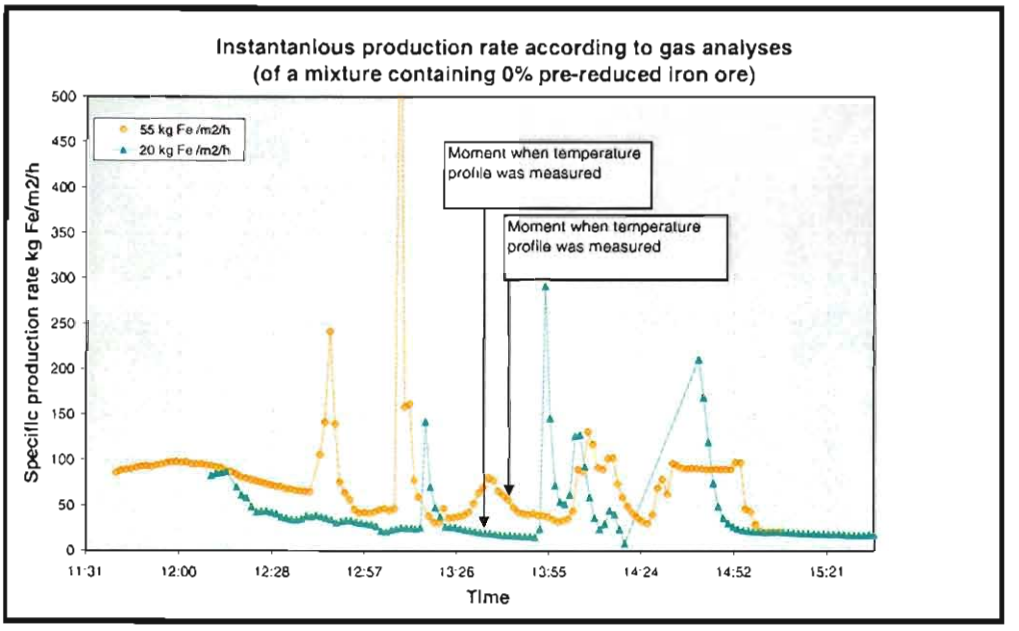

Figure 49: *Specific production rate calculated from gas analyses for tests done with material containing 0% pre-reduced iron ore.*

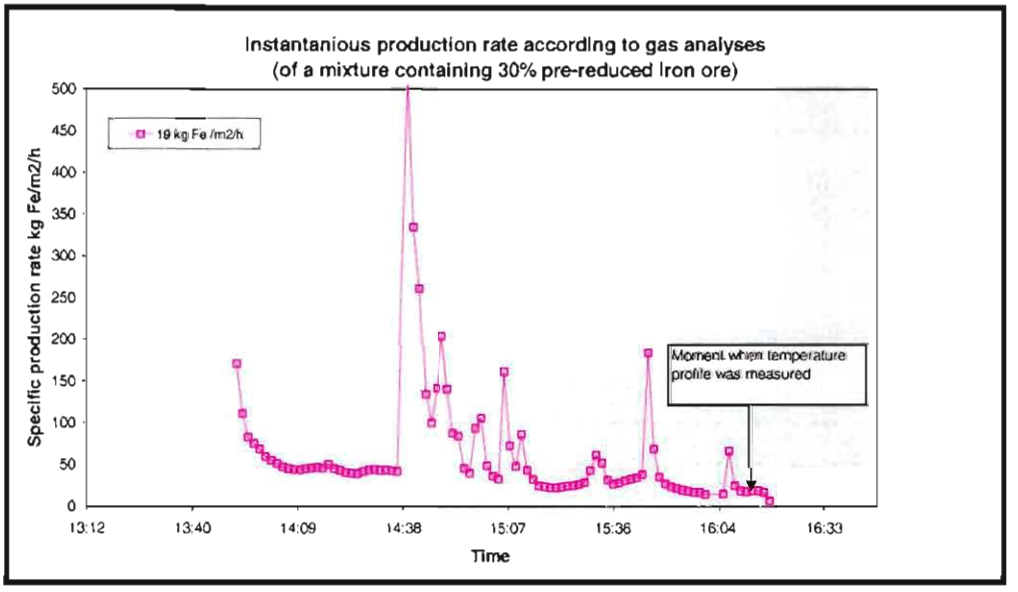

Figure 50: *Specific production rate calculated from gas analyses for tests done with material containing 30% pre-reduced iron ore.*

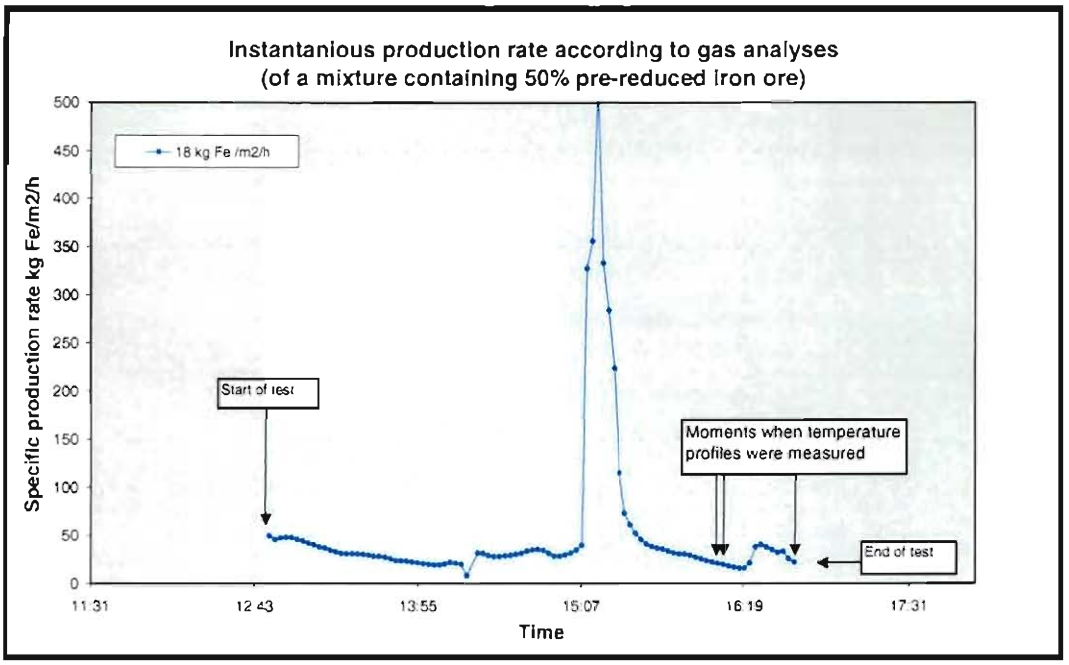

Figure 51: *Specific production rate calculated from gas analyses for tests done with material containing 50% pre-reduced iron ore.*

Figure 49, ***Figure 50*** and ***Figure 51*** show that sudden increases in the production rate from time to time. These increases were mostly observed as slag reactions occurring when part of the solids bed collapsed into the liquid bath.

Times when temperature profiles were measured are also shown in the figures above. From the figures, the actual production rate at the time of the measurement can be seen. These production rates were used as inputs to the model for predicting of the theoretical temperature profiles of the solids bed.

3.4.3.3 Model predictions vs experimental measurements

Figure 52 shows that experimental measurements were repeatable.

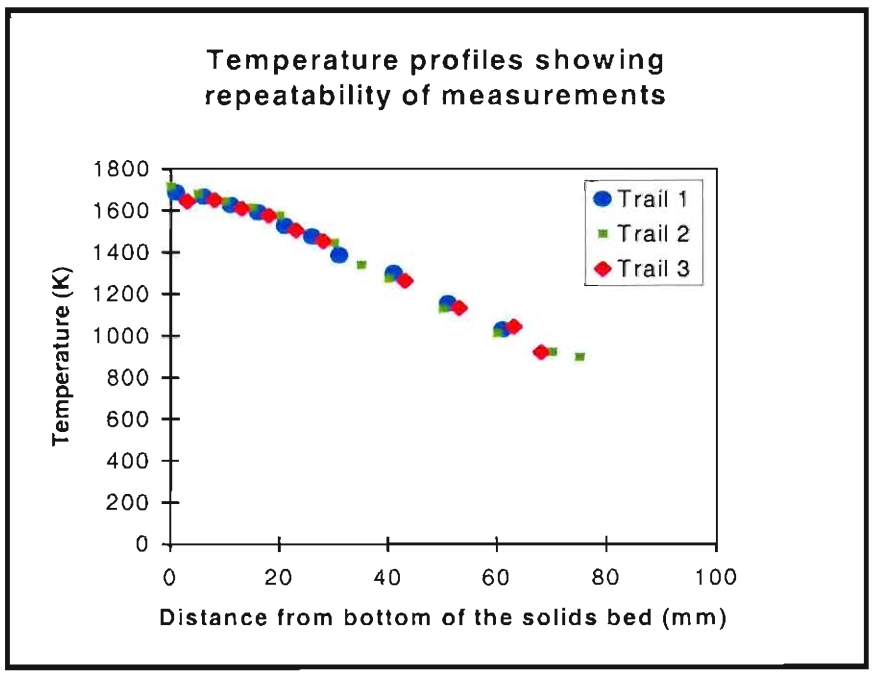

Figure 52: *Experimentally measured temperature profiles of the solids bed, showing repeatability of results. These tests were done with material containing 50% pre-reduced iron ore at a production rate of 18 kg Fe/m^2/h.*

Figure 52 shows that good repeatability of temperature profile measurements were achieved.

Measured temperature profiles are shown in ***Figure 53*** to ***Figure 56***. These figures also show the model simulations of the respective tests. Each test was individually modelled. The production rate and bath temperature that was measured during the test were used as inputs to the model. The model predicted the temperature profile as well as the reduction profile through the solids bed for the specific test.

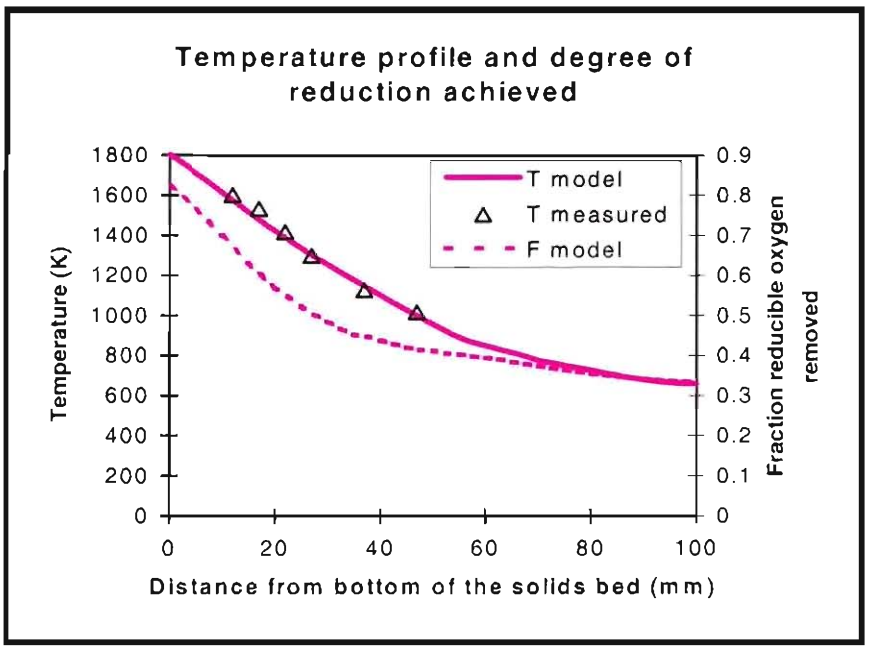

Figure 53: *Comparison between model prediction and experimentally measured temperature profiles of solids bed for a tests done with material containing 30% pre-reduced iron ore at a production rate of 19 kg Fe/m^2/h.*

Figure 53 shows a good correlation between the temperature profile predicted by the model and the actual measured profile. For this test the model predicted that 83% reduction would have been achieved at a production rate of 19 kg Fe/m2/h.

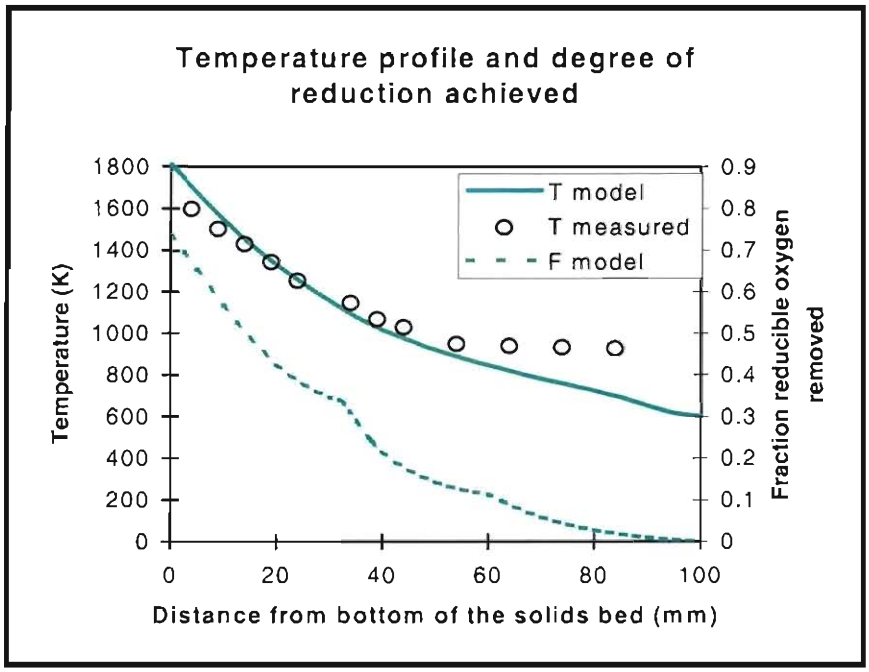

Figure 54: *Comparison between model prediction and experimentally measured temperature profiles of solids bed for a tests done with material containing 0% pre-reduced iron ore at a production rate of 20 kg Fe/m^2/h.*

Figure 54 shows a fair correlation between the temperature profile predicted by the model and the actual measured temperature profile.

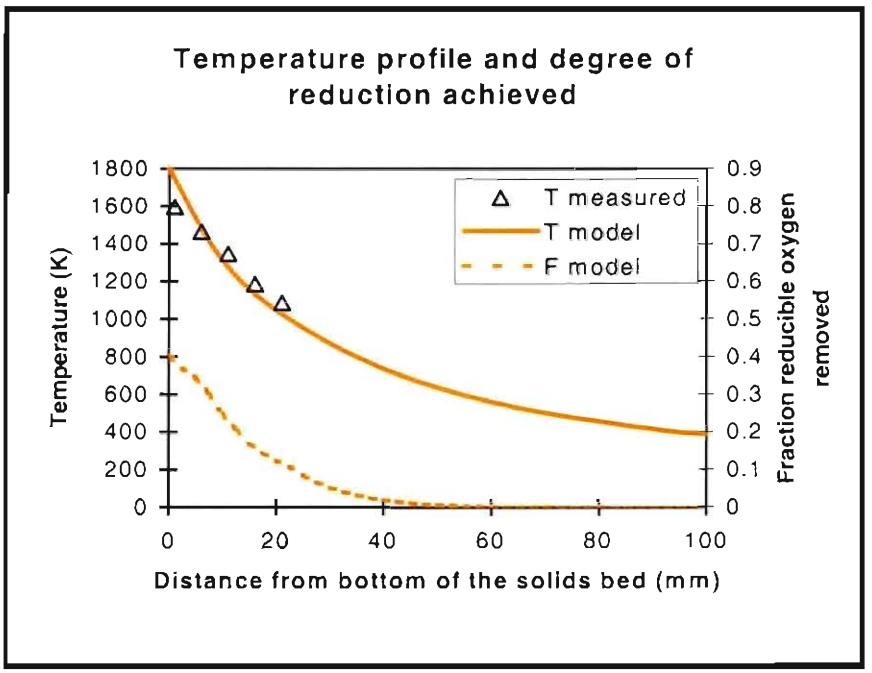

Figure 55: *Comparison between model prediction and experimentally measured temperature profiles of solids bed for a tests done with material containing 0% pre-reduced iron ore at a production rate of 55 kg Fe/m^2/h.*

Figure 55 shows the comparison between the temperature profile predicted by the model and the temperature profile that was measured during the test. The slope of the measured profile is slightly more horizontal than predicted by the model. This is ascribed to movement of the solids bed, due to large amounts of gas being generated below the bed.

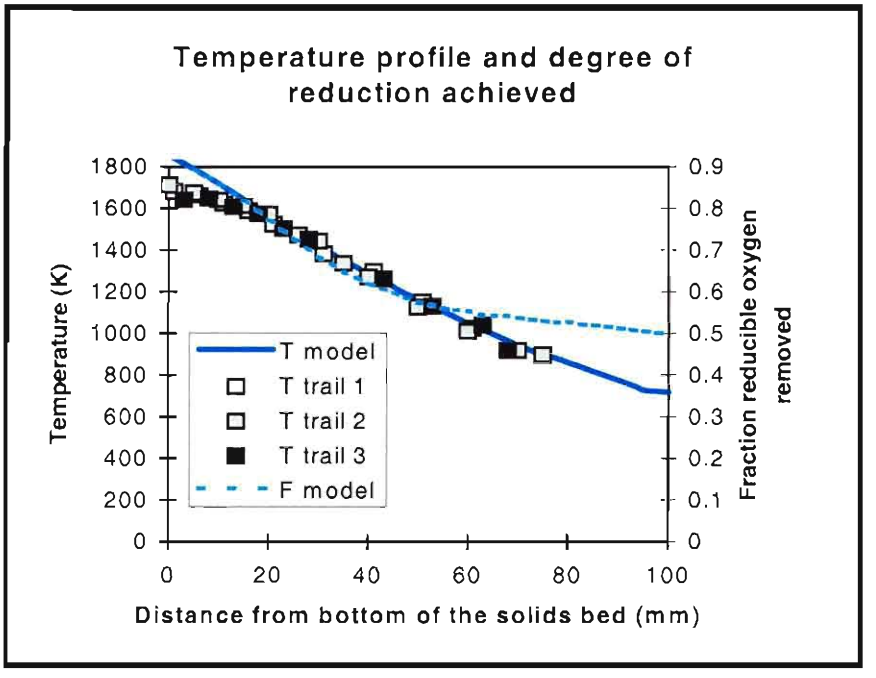

Figure 56: *Comparison between model I prediction and experimentally measured temperature profiles of solids bed for a tests done with material containing 50% pre-reduced iron ore at a production rate of 18 kg Fe/m^2/h.*

Figure 56 shows a good correlation between the temperature profile predicted by the model and the measured temperature profile. The model predicted 92% reduction achieved at the bottom of the solids bed.

3.4.4 Prediction of extent of reduction achieved.

From the previous paragraph it is evident that model predictions were similar to experimental measurements. The model was therefore used to predict the extent of reduction achieved at the bottom of the solids bed, for various degrees of reduction achieved in the upper part of the solids bed. This was done for different production rates, as shown in ***Figure 57***. A "dead zone" temperature of 700°C was assumed for these calculations.

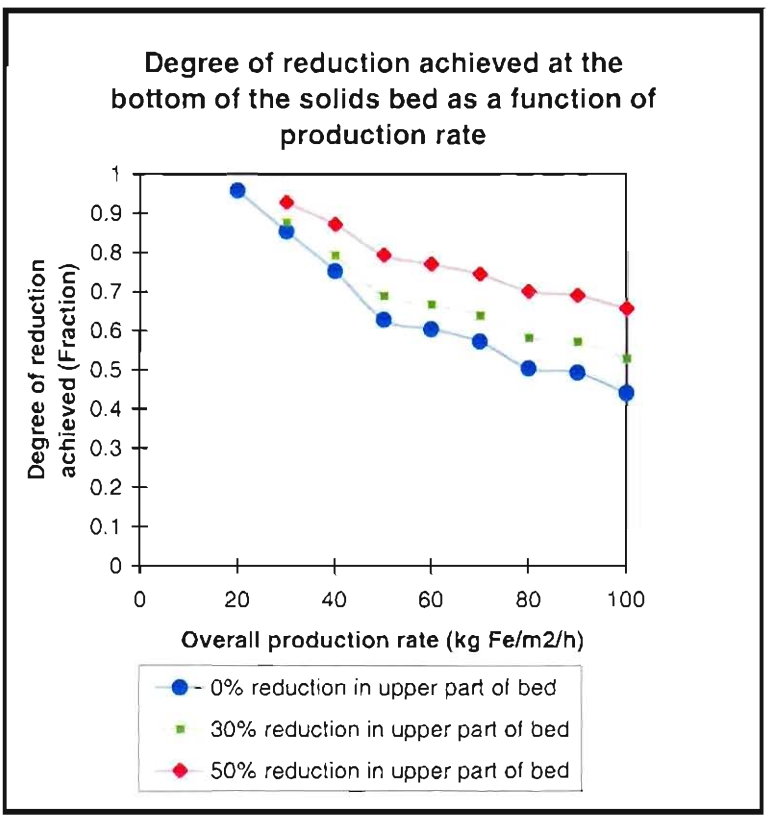

Figure 57: *Model prediction of reduction achieved at the bottom of the solids bed, for various degrees of reduction achieved in the upper part of the solids bed.*

Figure 58 shows the information of ***Figure 57*** fitted onto ***Figure 29.*** ***Figure 58*** therefore compares the degree of reduction achieved in the top part of the solids bed with the total amount of reduction achieved at the bottom of the solids heap, as a function of production rate.

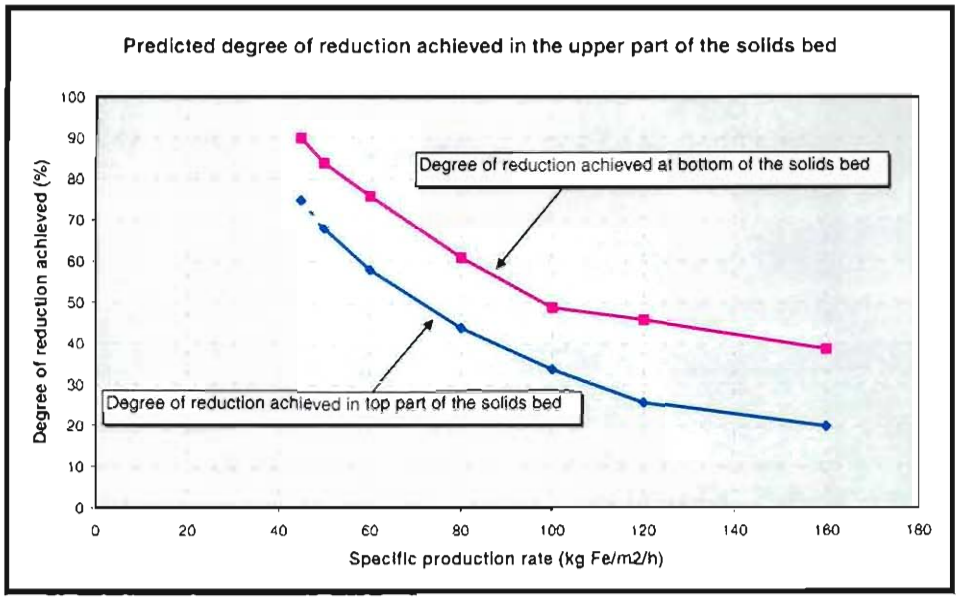

Figure 58: *Anticipated degree of reduction achieved in the upper part of the solids bed (when feeding 40 mm thick batches and with a freeboard temperature of 1500C) as well as the amount of reduction achieved at the bottom of the solids bed.*

At the Ifcon pilot plant facility steel was produced at a rate of 100 kg $Fe/m^2/h$[10,13,16,17]. ***Figure 58*** shows that the anticipated amount of reduction achieved in the upper part of the solids bed was 34 % for a production rate of 100 kg $Fe/m^2/h$, and 49% at the bottom of the solids bed. At a production rate of 100 kg $Fe/m^2/h$, the ore is therefore not fully reduced when reaching the bottom of the solids bed. This implies that final reduction in the Ifcon process did not occur as solid-state reduction. Slag metal reactions therefore must be considered during operation of the Ifcon process.

Since the aim is to achieve 90% reduction in the Ifcon process, the maximum degree of reduction that will be achieved at the top of the solids bed (for these specific conditions) is about 75% at a production rate of 45 kg/m2/h. This is an extrapolated value.

3.5 Conclusions:

In response to technology drivers in the iron and steel industry, various direct reduction- and direct smelting processes were developed. One of these is the Ifcon process, which produces liquid crude steel directly from raw materials.

The reduction rate is significantly increased when the exposure temperature is increased. The presence of volatile matter (in the coal) also increases the rate at which reduction is achieved.

When selecting the optimum feed materials for the process, **ore and coal** should not only be selected according to chemical composition but also according to CO reducibility and CO_2 reactivity. The effect of these parameters on the overall reduction rate is however limited.

The degree of reduction achieved at the bottom of the solids bed (with the current material mixture) depends on the following factors:

- the rate constant of the reduction reaction.
- The thermal conductivity of the solids bed.
- the temperature of the metal bath.
- the production rate .
- the degree of reduction achieved in the upper part of the solids bed.

At a production rate of 100 kg Fe/m^2/h the ore is not fully reduced at the bottom of the solids bed. At this production rate solid-liquid-state reduction accounts for approximately 41% of the total reduction achieved, assuming a final degree of reduction of 90%.

The above only gives insight to the extent to which reactions occur in the solids bed of the process. In order to comment on the final degree of reduction achieved (and production rate), the rate and extent to which solid-liquid-state reduction occurs must be taken into account.